Mixed-Gas Adsorption

Flor R. Siperstein and Alan L. Myers
Dept. of Chemical Engineering, University of Pennsylvania, Philadelphia, PA 19104

The prediction of multicomponent adsorption equilibria from single-component data is one of the most challenging and important problems in adsorption. The chief obstacle to progress is a scarcity of accurate and consistent experimental data over a wide range of temperature and loading for testing theories. Several binaries and one ternary system on two types of zeolites (silicalite and faujasite) were studied in a combination calorimeter-volumetric apparatus. Activity coefficients and excess functions for enthalpy, free energy, and entropy were extracted from the binary data using a three-constant equation to represent nonidealities. The successful correlation of binary excess functions with pure-component properties for type I isotherms on zeolites is a first step toward predicting multicomponent adsorption from single-gas adsorption and a major advancement over the theory of ideal adsorbed solutions.

Introduction

The ability of porous materials to adsorb fluids selectively is the basis of many industrial applications, especially catalysis and the separation and purification of gases and liquids. Industrial applications of adsorption include the recovery of organic solvent vapors, dehydration of gases, separation and purification of hydrogen from steam-methane reformers, separation and purification of air, separation of normal paraffins from branch and cyclic paraffins, production of olefins from olefin and paraffin mixtures, and so on (Tien, 1994; Crittenden and Thomas, 1998; Yang, 1987). Even though adsorption plays an important role in the gas separation and purification industry, the prediction of multicomponent equilibria is still one of the most challenging problems in adsorption (Talu, 1998).

The main problem is a lack of accurate and consistent experimental data for testing theories. Almost no data are available on enthalpy of adsorbed mixtures, although such information is necessary for the modeling of fixed-bed adsorbers. Indirect measurements of mixture heats of adsorption using volumetric or gravimetric methods are possible in principle, but require voluminous data on isobars, isotherms, and loci of constant composition (Sircar, 1985, 1991).

Experimentally, an isotopic, steady-state kinetic technique was used to calculate mixture heats of adsorption (Bajusz et al., 1998a,b). Other studies have used the isosteric method to measure mixture equilibria (Bülow, 1994; Bülow and Shen, 1998; Hampson and Rees, 1993; Rees et al., 1991). We have described previously a calorimeter for simultaneous measurements of mixture equilibria and heats of adsorption (Dunne et al., 1997; Siperstein et al., 1999a). Here, we report activity coefficients, excess free energies, and enthalpies of mixing in the adsorbed phase.

The objective of this article is to understand the molecular basis for these deviations from ideality and attempt to predict them on the basis of single-gas properties. Deviations from ideal mixing are expressed as excess functions: excess free energy (activity coefficients) and excess enthalpy (deviations from ideal enthalpy of mixing). This excess function approach is analogous to standard methods for expressing nonideal behavior in liquid mixtures (Prausnitz et al., 1999). However, the use of excess functions for describing deviations from ideal mixing in the adsorbed phase differs from liquid solutions in several subtle but important ways, especially in how these excess functions are measured experimentally.

Enthalpy and Heat of Adsorption

The standard procedure for studying adsorption equilibrium is to measure loading at several temperatures. Typically, three adsorption isotherms are measured at intervals of 30°C so that the behavior of the system is determined within a band of 60°C, a region ± 30°C from the middle isotherm. Our volumetric-calorimetric method is the simultaneous measurement of a single isotherm and the heat of adsorption, so that the temperature dependence within some interval of temperature is provided by thermodynamic equations linked to the heat of adsorption. It is estimated that the assumption of constant heat of adsorption over a temperature interval of ± 30°C from a reference temperature generates errors less than 1% in pressure and loading (Shen et al., 2000).

Correspondence concerning this article should be addressed to A. L. Myers.

The calorimetric method, which has been applied to single component adsorption (Dunne et al., 1996a,b; Sircar et al., 1999) and to mixture adsorption (Dunne et al., 1997; Siperstein et al., 1999b), reduces the experimental effort for mixtures without sacrifice of accuracy. The calorimetric method is also ideally suited to the measurement of thermodynamic excess functions such as enthalpy of mixing of adsorbed solutions.

Fundamental equations for differential enthalpy

The heat of adsorption mentioned most frequently is the isosteric heat (Valenzuela and Myers, 1989)

$$q_{st} = RT^2\left(\frac{\partial \ln P}{\partial T}\right)_n \tag{1}$$

which is evaluated by differentiating single-gas adsorption isotherms at constant loading (n). q_{st} is a positive quantity and $q_{st}\,dn$ is the differential heat liberated by the isothermal desorption of a differential amount of adsorbate dn. Unfortunately, the terminology ''heat of adsorption'' is vague and there is disagreement in the literature about its definition. Equation 1, which is for adsorption from a pure perfect gas, needs to be extended to the general case of adsorption from a real gas mixture. The heat of adsorption measured experimentally depends upon the imposed conditions: batch, steady state, isothermal, isobaric, and so on. The existence of several different types of heats of adsorption (equilibrium, integral, differential, and isosteric) adds to the confusion. Instead of insisting upon a particular path for the generalized definition of isosteric heat, it is advantageous to work with differential and integral enthalpies which are state variables and therefore independent of the path.

Let H^m be the experimental (Gibbs excess) enthalpy of an adsorbed gas mixture containing n_1^m moles of component 1, n_2^m moles of component 2, and so on. The superscript m signifies ''measured'' by conventional volumetric, gravimetric, or calorimetric methods. The superscript m on the mol numbers (n_i^m) will be omitted to simplify notation. H^m is the integral enthalpy in units of joules per kilogram of adsorbent. Let h_i^* be the molar enthalpy of component i in the pure, perfect gas state at the same temperature as the mixture. The integral enthalpy of desorption relative to the perfect-gas reference state is

$$\Delta H = \sum_i n_i h_i^* - H^m \tag{2}$$

Stated differently, $-\Delta H$ is the integral enthalpy of the adsorbed phase relative to the perfect-gas reference state. Since desorption is normally an endothermic process, ΔH is a positive quantity. The molar integral enthalpy of desorption is then

$$\Delta h = \frac{\Delta H}{n_t} = \sum_i x_i h^* - \frac{H^m}{n_t} \tag{3}$$

where total loading is

$$n_t = \sum_i n_i \tag{4}$$

and $x_i = n_i/n_t$ is the mol fraction of ith component in the adsorption phase.

The differential enthalpy of desorption of the ith component is

$$\Delta \bar{h}_i = \left[\frac{\partial \Delta H}{\partial n_i}\right]_{T,n_j} = h_i^* - \left[\frac{\partial H^m}{\partial n_i}\right]_{T,n_j} \tag{5}$$

If the differential enthalpy is measured by calorimetry, the molar integral enthalpy (heat of immersion) may be obtained by integration

$$\Delta h = \frac{\int_0^{n_t} \sum_i \left(\Delta \bar{h}_i\, dn_i\right)}{n_t} \tag{6}$$

Integral enthalpy is a state function and therefore the integration of Eq. 6 is independent of the path. Even for single-gas adsorption, Eq. 6 shows that the integral enthalpy is not equal to the differential enthalpy unless the latter is independent of loading.

Equation 1 is extended to the general case of a real gas mixture in Appendix A. The result for the differential enthalpy of the ith component relative to its perfect-gas reference state is

$$\Delta \bar{h}_i = RT^2\left(\frac{\partial \ln f_i}{\partial T}\right)_{n_1,n_2,\ldots} \tag{7}$$

This exact relation allows differential enthalpies to be calculated from adsorption isotherms. For a perfect gas, $f = P$ and

$$\Delta \bar{h} = RT^2\left(\frac{\partial \ln P}{\partial T}\right)_n \tag{8}$$

Comparison of Eqs. 1 and 8 shows that $q_{st} = \Delta \bar{h}$ for the special case of a pure perfect gas. The differential enthalpy defined by Eqs. 5 and 7 is needed for the description of mixture adsorption. The actual heat of adsorption can always be calculated from the differential enthalpy once the path is specified.

Summary of equations for adsorption equilibrium

For adsorption of a gas mixture containing N_c components, the equilibrium condition is equality of fugacity in the adsorbed and gas phases (Myers and Prausnitz, 1965)

$$Py_i\phi_i = f_i^\circ x_i \gamma_i \qquad (i = 1, 2, \ldots, N_c) \tag{9}$$

where P is pressure, y and x are mol fractions in the gas and adsorbed phase, respectively, ϕ_i is the fugacity coefficient of component i in the gas phase, f_i° is the fugacity of the pure component in its standard state, and γ_i is the activity coefficient of component i in the adsorbed phase.

The standard state is fixed by the surface potential (Φ), which for a pure component is

$$\Phi = -RT\int_0^P n\, d\ln f \qquad (\text{constant } T) \tag{10}$$

The condition for applying the fugacity equations is that the fugacities of the pure components (f_i°) be evaluated at the surface potential (Φ) of the mixture. For a pure perfect gas, fugacity (f) is equal to pressure (P) and

$$\Phi = -RT\int_0^P n d\ln P \qquad \text{(constant } T\text{)} \tag{11}$$

The reason for defining the standard state in terms of the surface potential is that the fugacity equations obey the rules of thermodynamic consistency, especially the Gibbs adsorption isotherm

$$d\Phi = -\sum_i n_i d\mu_i \qquad \text{(constant } T\text{)} \tag{12}$$

The Gibbs free energy of the adsorbed phase is

$$G = \sum_i \mu_i n_i + \Phi \tag{13}$$

The surface potential has traditionally been expressed as $\Phi = -\Pi A$, the product of a two-dimensional (2-D) spreading pressure (Π) and specific surface area (A). The quantities Π and A can only be estimated in pores, but their product is given exactly by Eq. 10. Equation 13 shows that the surface potential is actually the chemical potential of the solid adsorbent relative to its pure state *in vacuo* at the same temperature.

The extensive variables G and n_i in Eq. 13 are experimentally ''measured'' Gibbs surface excess variables which could be emphasized by the notation G^m and n_i^m, but the superscripts have been omitted in the interest of simplifying the notation.

As shown later, a variable which arises frequently in adsorption thermodynamics is

$$\psi = -\frac{\Phi}{RT} = \int_0^P n d\ln f = \int_0^n \left(\frac{\partial \ln f}{\partial \ln n}\right)_T dn \qquad \text{(constant } T\text{)} \tag{14}$$

Since the surface potential (Φ) has units of J/kg, ψ has units of mol/kg, the same as loading.

It is convenient to define the excess free energy of the adsorbed solution by

$$g^e = RT\sum_i^{N_c} x_i \ln \gamma_i \tag{15}$$

In Eq. 15 and in the equations to follow, the superscript e refers to excess functions, as commonly defined in solution thermodynamics of liquid mixtures (Prausnitz et al., 1999) and is not to be confused with Gibbs surface excess variables; all extensive variables in the adsorbed phase (G, H, S, n_i) are Gibbs surface excess variables. The g^e function refers to the Gibbs free energy of the adsorbate species exclusive of the solid, the quantity ($G - \Phi$) in Eq. 13. This special definition of g^e allows adsorbed-phase activity coefficients to be expressed as partial-molar derivatives in the customary way

$$RT\ln\gamma_i = \left[\frac{\partial(n_t g^e)}{\partial n_i}\right]_{T,\psi,n_j} \tag{16}$$

Note that the variables held constant for the differentiation are temperature and ψ, unlike the partial molar quantities of solution thermodynamics for which temperature and pressure are fixed. Let the excess reciprocal loading be defined as

$$(1/n)^e + \frac{1}{n_t} - \sum_i^{N_c}\left[\frac{x_i}{n_i^\circ}\right] \tag{17}$$

The excess reciprocal loading vanishes for an ideal solution. It can be shown (Talu et al., 1995) that Eqs. 15 and 17 are related by

$$(1/n)^e = \left[\frac{\partial(g^e/RT)}{\partial\psi}\right]_{T,x} \tag{18}$$

The selectivity of the adsorbent for component 1 relative to component 2 is a commonly used measure of separation power; using Eq. 9

$$s_{1,2} = \frac{x_1/y_1}{x_2/y_2} = \frac{f_2^\circ\gamma_2/\phi_2}{f_1^\circ\gamma_1/\phi_1} \tag{19}$$

Differential enthalpy from activity coefficients and excess reciprocal loading

Equations 9 to 19 describing the equilibria of adsorbed solutions have been published previously (Valenzuela and Myers, 1989). Here, equations are derived for the differential enthalpy of desorption (isosteric heat) in order to introduce the temperature variable in a systematic way. For the general case of a multicomponent real gas and a nonideal adsorbed solution, it is shown in Appendix B that the differential enthalpy of desorption of the ith component is equal to

$$\Delta\bar{h}_i = \Delta h_i^\circ + RT^2\left(\frac{\partial\ln\gamma_i}{\partial T}\right)_{\psi,x} + \left[\frac{1}{n_i^\circ} + \left(\frac{\partial\ln\gamma_i}{\partial\psi}\right)_{T,x}\right] \times \left[\frac{\sum_j x_j G_j^\circ n_j^\circ\left(\Delta\bar{h}_j^\circ - \Delta h_j^\circ\right) + RT^2\left(\frac{\partial(1/n)^e}{\partial T}\right)_{\psi,x}}{\sum_j x_j G_j^\circ - \left(\frac{\partial(1/n)^e}{\partial\psi}\right)_{T,x}}\right] \tag{20}$$

where

$$G_i^\circ \equiv \frac{1}{(n_i^\circ)^2}\left(\frac{\partial\ln n_i^\circ}{\partial\ln f_i^\circ}\right)_T \tag{21}$$

This rigorous equation gives the mixture differential enthalpy ($\Delta\bar{h}_i$) in terms of the pure-component differential enthalpy ($\Delta\bar{h}_i^\circ$), the pure-component integral enthalpy (Δh_i°), and the variation of the activity coefficient (γ_i) and excess reciprocal loading $(1/n)^e$ with respect to temperature and ψ. As in the

case of the fugacity equations, the surface potential ($\Phi = -RT\psi$) plays the essential role of connecting mixture heats with their single-component values.

For the special case of an ideal solution, for which $\gamma_i = 1$ and $(1/n)^e = 0$, Eq. 20 simplifies to (Karavias and Myers, 1991)

$$n_i^\circ\left(\Delta\bar{h}_i - \Delta h_i^\circ\right) = \frac{\sum_j x_j G_j^\circ n_j^\circ\left(\Delta\bar{h}_j^\circ - \Delta h_j^\circ\right)}{\sum_j x_j G_j^\circ} \qquad (22)$$

For example, the differential enthalpy of component 1 in a binary solution of components 1 and 2 is

$$\Delta\bar{h}_1 = \Delta h_1^\circ + \frac{1}{n_1^\circ} \times \left[\frac{x_1 G_1^\circ n_1^\circ\left(\Delta\bar{h}_1^\circ - \Delta h_1^\circ\right) + x_2 G_2^\circ n_2^\circ\left(\Delta\bar{h}_2^\circ - \Delta h_2^\circ\right)}{x_1 G_1^\circ + x_2 G_2^\circ}\right] \qquad (23)$$

If the differential enthalpies for single-gas adsorption are all constant (independent of loading), it follows from Eq. 6 that the integral and differential enthalpies are equal. For this rare case, Eq. 22 predicts that the mixture differential enthalpies for an ideal solution are equal to their (constant) pure component values.

Equations 20 and 22 cannot be simplified for the usual case when the differential enthalpy of the pure gas varies with loading. The empirical approximation that the mixture differential enthalpy is equal to the value for the pure component at the same loading appears to have no theoretical basis.

Thermodynamic Model

A three-constant model of binary adsorption is proposed. All of the equilibrium properties of the mixture may be calculated from the excess Gibbs free energy

$$g^e = (A + BT)\, x_1 x_2 (1 - e^{-C\psi}) \qquad (24)$$

where A, B, and C are constants. Equation 24 is called the ABC equation to emphasize that it contains three constants which are independent of temperature, loading, and composition. This equation is the simplest form with the built-in limits required of any theory (Talu and Myers, 1988; Valenzuela and Myers, 1989), especially thermodynamic consistency and reduction to an ideal adsorbed solution at the limit of zero loading. Specifically, the constant A is proportional to the excess enthalpy, the constant B is proportional to the excess entropy, and the constant C is proportional to the excess reciprocal loading. The exponential dependence upon ψ (defined by Eq. 14) agrees with experiment and molecular simulation from zero loading up to saturation (Talu et al., 1995). Although the excess free energy has a quadratic (symmetrical) composition dependence at constant ψ in Eq. 24, the composition dependence at constant pressure has the asymmetrical form observed experimentally. The linear dependence of excess free energy upon temperature implies an enthalpy which is independent of temperature, an approximation consistent with the customary assumption that the differential enthalpies (''heats'') are constant over the temperature range of interest.

The excess reciprocal loading is obtained by inserting Eq. 24 into Eq. 18

$$(1/n)^e = \left(\frac{\partial g^e/RT}{\partial\psi}\right)_{T,x} = \frac{C}{RT}(A + BT)\, x_1 x_2 e^{-C\psi} \qquad (25)$$

This excess function is needed to calculate the total loading (n_t) from Eq. 17. According to Eq. 17, $\lim_{n_t \to 0}(1/n)^e = (\infty - \infty)$, which is a finite but non-zero limit (Talu et al., 1995). The finite limit ($\psi \to 0$) from Eq. 25 is correct and consistent with setting $(1/n)^e = 0$ for ideal solutions at the limit of zero loading.

Equation 25 predicts that the limit of $(1/n)^e$ is zero at the saturation capacity ($\psi \to \infty$) of the adsorbent.

The activity coefficients are given by substituting Eq. 24 into Eq. 16

$$RT \ln \gamma_i = (A + BT)(1 - e^{-C\psi})\, x_j^2 \qquad (i \neq j) \qquad (26)$$

This equation satisfies the requirement that the activity coefficient be unity at the limit of zero loading ($\psi \to 0$). At high loading ($\psi \to \infty$), the activity coefficient approaches a constant value corresponding to saturation.

The four partial derivatives needed in Eq. 20 were calculated from Eqs. 25 and 26

$$\left(\frac{\partial \ln \gamma_i}{\partial T}\right)_{\psi,x} = -\frac{A}{RT^2}(1 - e^{-C\psi})\, x_j^2 \qquad (i \neq j) \qquad (27)$$

$$\left(\frac{\partial \ln \gamma_i}{\partial \psi}\right)_{T,x} = \frac{(A + BT)}{RT} C e^{-C\psi} x_j^2 \qquad (i \neq j) \qquad (28)$$

$$\left(\frac{\partial (1/n)^e}{\partial T}\right)_{\psi,x} = -\frac{AC}{RT^2} x_1 x_2 e^{-C\psi} \qquad (29)$$

$$\left(\frac{\partial (1/n)^e}{\partial \psi}\right)_{T,x} = -\frac{(A + BT)}{RT} C^2 x_1 x_2 e^{-C\psi} \qquad (30)$$

Application of the Gibbs-Helmholtz relation to Eq. 24 yields

$$h^e = -T^2 \frac{\partial}{\partial T}\left[\frac{g^e}{T}\right]_{\psi,x} = A x_1 x_2 (1 - e^{-C\psi}) \qquad (31)$$

Physically, the excess enthalpy is the molar enthalpy of mixing of the adsorbed solution at constant surface potential. Note that the enthalpy of mixing is independent of temperature for our model, which is consistent with the assumption that differential enthalpies (heats) are independent of temperature.

Multicomponent systems

In preparation for a discussion of experimental data obtained for a ternary mixture, the previous equations for the binary case are next extended to a multicomponent mixture. Our assumption of a quadratic composition dependence for the excess functions implies the dominance of pairwise inter-

actions, so that the ABC equation for a multicomponent system (ternary and higher) is additive in the constituent binaries (Walas, 1984). The excess free energy can be written

$$g^e = \sum_{i=1}^{Nc} \sum_{j=1}^{Nc} \left(A_{ij} + B_{ij}T \right) x_i x_j (1 - e^{-C_{ij}\psi})(j > i) \quad (32)$$

where A_{ij}, B_{ij}, and C_{ij} are the binary parameters for the ABC equation. Specifically, for a ternary mixture

$$\begin{aligned} g^e = &\left(A_{12} + B_{12}T \right) x_1 x_2 (1 - e^{-C_{12}\psi}) \\ &+ \left(A_{13} + B_{13}T \right) x_1 x_3 (1 - e^{-C_{13}\psi}) \\ &+ \left(A_{23} + B_{23}T \right) x_2 x_3 (1 - e^{-C_{23}\psi}) \end{aligned} \quad (33)$$

Experimental Studies

Materials

Two types of zeolites were studied, silicalite and NaX (FAU). The structures and compositions of these materials are very different. Silicalite has a unit cell composition of $Si_{96}O_{192}$ and contains straight and sinusoidal channels with pore openings of 5.3×5.6 and 5.1×5.5 Å, respectively. FAU has a unit cell composition of $Na_{86}Al_{86}Si_{106}O_{384}$ and contains 15 Å-diameter supercages interconnected by 7.4 Å-diameter windows in a tetrahedral arrangement (Meier and Olson, 1992). Silicalite provides a homogeneous environment for both polar and nonpolar molecules, whereas polar molecules exhibit energetic heterogeneity in NaX due to the presence of nonframework sodium ions.

We used commercial powders of these zeolites: silicalite (Linde S115) manufactured by Union Carbide Corp. and NaX (Linde 13X) with a Si/Al ratio of 1.23. Thermogravimetric analysis of the samples yielded dehydrated weights of 99% and 76% of that in air, respectively (Dunne et al., 1996a,b).

Gases used in the experiments were from Air Products & Chemicals, Inc. (SF_6, 99.99%; C_2H_4, 99.5%; C_2H_6, 99%; C_3H_8, 99.5%) and from Airco (CO_2, 99.99%; CH_4, 99.99%).

Method

The multicomponent calorimeter and the experimental procedure have been described previously in detail (Dunne et al., 1997; Siperstein et al., 1999a).

The pretreatment procedure for the sample was heating *in situ* under vacuum from room temperature to 110°C over 24 h for a fresh sample, or 12 h when regenerating a used sample. This is followed by heating over a period of 12 h from 110°C to 350°C and, finally, maintaining the temperature at 350°C for 12 h.

For binary and ternary mixture measurements, the components were dosed alternately in order to measure the mixture enthalpies. The composition of the equilibrium gas was measured with a mass spectrometer through a leak valve attached to the sample cell. Loadings of both components were calculated from mass balances using standard volumetric procedures. The attainment of equilibrium was verified by reversing the order in which the components were added to the sample cell.

Analysis of Experimental Data

The seven binary mixtures listed in Table 1 cover behavior ranging from nearly ideal to highly nonideal. NaX is classified as heterogeneous because of the high electric field strength associated with its exchangeable cations; silicalite is classified as homogeneous because it has no exchangeable cations and a relatively low electric field strength. Partial results for some of these systems reported previously are indicated by the reference in Table 1. The experimental data are tabulated in Appendix C.

Single-gas isotherms and isosteric heats

Calculations of mixture properties such as adsorbed-phase activity coefficients are extremely sensitive to the properties of the single adsorbates. For this reason, we devoted special attention to the reproducibility of the experimental data. Reversibility was established by comparing points obtained by adsorption and desorption. Single gas isotherms are shown in Figures 1 and 2. The three experimental points in Figure 2 for CH_4 on silicalite at pressures above 1 bar from Golden and Sircar (1994) are needed to extrapolate our data to high pressure for mixture calculations.

In preparation for calculating thermodynamic properties, the single gas isotherms were fitted with a modified virial equation

$$HP = n\left[\frac{m}{m-n} \right] \exp\left[C_1 n + C_2 n^2 + C_3 n^3 + C_4 n^4 \right] \quad (34)$$

Constants for Eq. 34 are given in Table 2. The virial equation extrapolates properly to zero pressure: $\lim_{P \to 0}(dn/dp) = H$. The factor $m/(m-n)$ was added to enforce Langmuirian behavior at high pressure where the virial expansion used by itself diverges. Thus, Eq. 34 has the correct asymptotic behavior at high and low pressure plus sufficient flexibility to fit all of the isotherms within experimental error. The average difference between the experimental pressure and the value calculated by Eq. 34 is 1.1%.

Table 1. Binary Gas Mixtures Studied

Type of System	Adsorbent	Gas 1	Gas 2	Ref.
Homogeneous, size difference	Silicalite	SF_6	CH_4	Siperstein et al. (1999a)
Homogeneous, ideal	Silicalite	C_2H_6	CH_4	Dunne et al. (1997)
Heterogeneous, polar-nonpolar	NaX	CO_2	C_2H_6	Dunne et al. (1997)
Heterogeneous, polar-nonpolar	NaX	CO_2	C_3H_8	
Heterogeneous, polar-nonpolar	NaX	C_2H_4	C_2H_6	Siperstein et al. (1999b)
Heterogeneous, nonpolar-nonpolar	NaX	SF_6	C_2H_6	
Heterogeneous, polar-polar	NaX	CO_2	C_2H_4	

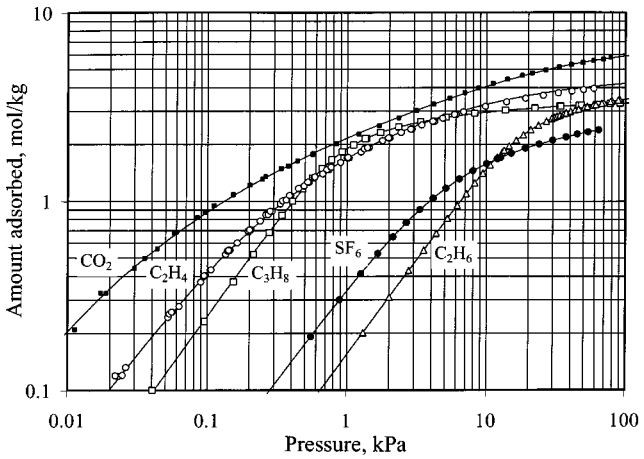

Figure 1. Experimental adsorption isotherms on NaX.

CO_2 at 293 K (■); C_2H_4 at 293 K (○); C_3H_8 at 293 K (□); SF_6 at 295 K (●); C_2H_6 at 293 K (△). Solid lines are Eq. 34 with constants from Table 2.

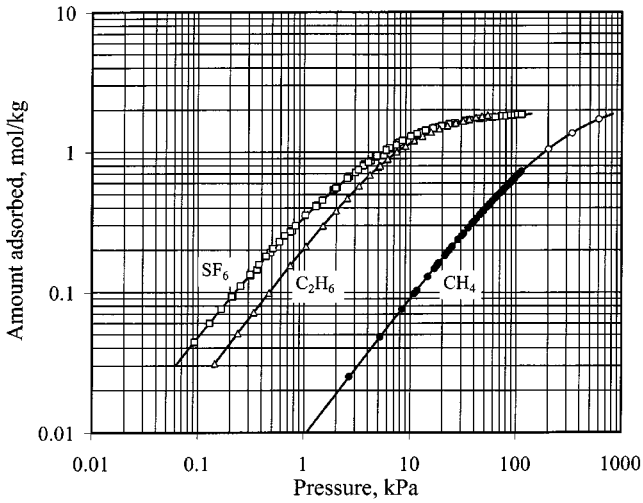

Figure 2. Experimental adsorption isotherms on silicalite.

SF_6 at 298 K (□); C_2H_6 at 296 K (△); CH_4 at 297 K (●). Data from Golden and Sircar (1994) for CH_4 (○). Solid lines are Eq. 34 with constants from Table 2.

The differential enthalpies (heats) of desorption shown in Figures 3 and 4 were fit by a Maclaurin series

$$\Delta\bar{h} = \Delta\bar{h}^\circ + \sum_{i=1}^{4} D_i n^i \tag{35}$$

Constants for Eq. 35 are given in Table 3. $\Delta\bar{h}^\circ$ is the limiting differential enthalpy at zero coverage. The average error between the experimental and calculated differential enthalpies is 1.3%.

Two different runs are reported in Table 3 for CO_2 on NaX. The heats for run II were made on a different sample of NaX and are about 2 kJ/mol higher; the single gas isotherms for these two runs were indistinguishable.

Substitution of Eq. 35 into Eq. 6 gives the molar integral enthalpy of desorption

$$\Delta h = \Delta\bar{h}^\circ + \sum_{i=1}^{4} \frac{D_i}{(i+1)} n^i \tag{36}$$

Binary mixtures

As pointed out before, the surface potential is needed for mixture calculations. Substitution of Eq. 34 into Eq. 14 and replacing fugacity (f) by pressure (P) gives for pure adsorbates

$$\psi(n) = \frac{1}{2}C_1 n^2 + \frac{2}{3}C_2 n^3 + \frac{3}{4}C_3 n^4 + \frac{4}{5}C_4 n^5 - m\ln\left(1 - \frac{n}{m}\right) \tag{37}$$

Using individual loadings (n_1, n_2) and temperature as independent variables for binary mixtures, the total loading is $n_t = (n_1 + n_2)$ and the composition of the adsorbed phase is $x_1 = n_1/n_t$. The surface potential in the mixture ($\psi = \psi_1^\circ = \psi_2^\circ$) was determined by combining Eqs. 17 and 25

$$(1/n)^e = \frac{1}{n_t} - \left[\frac{x_1}{n_1^\circ} + \frac{x_2}{n_2^\circ}\right] = \frac{C}{RT}(A + BT)\,x_1 x_2 e^{-C\psi} \tag{38}$$

Inversion of Eq. 37 yields the functions $n_1^\circ(\psi)$ and $n_2^\circ(\psi)$ at the common standard state (ψ). Substitution of these two functions into Eq. 38 yields a single equation in a single unknown (ψ). Having solved for ψ, the standard-state pressures (P_1° and P_2°) are given by Eq. 34. Adsorbed-phase activity coefficients are calculated from Eq. 26. Finally, Eq. 9 written

Table 2. Constants of Eq. 34 for Single Gas Isotherms*

Gas	Zeolite	H mol/(kg·kPa)	C_1	C_2	C_3	C_4	m mol/kg	T °C	Error %
CO_2	NaX	27.253	1.2338	−0.1241	0.0038	0.0	6.4674	20.0	3.0
C_3H_8	NaX	2.3657	−0.5251	0.3367	−0.2419	0.0648	3.4288	20.0	1.3
C_2H_4	NaX	5.2039	0.3850	0.0075	0.0012	0.0012	4.5341	20.0	1.6
C_2H_6	NaX	0.1545	−0.2670	−0.0499	0.0192	0.0	3.8937	20.0	0.2
SF_6	NaX	0.3623	−0.0661	−0.0491	0.1115	0.0	3.4393	22.3	0.2
SF_6	Silicalite	0.5010	0.8010	−0.7501	0.2357	0.0	1.9495	25.0	1.4
C_2H_6	Silicalite	0.2145	−0.2752	0.1272	0.0	0.0	2.1534	23.0	0.6
CH_4	Silicalite	0.00945	0.0837	−0.0470	0.0	0.0	2.4578	24.0	0.4

*P is given in kPa for n in mol/kg.

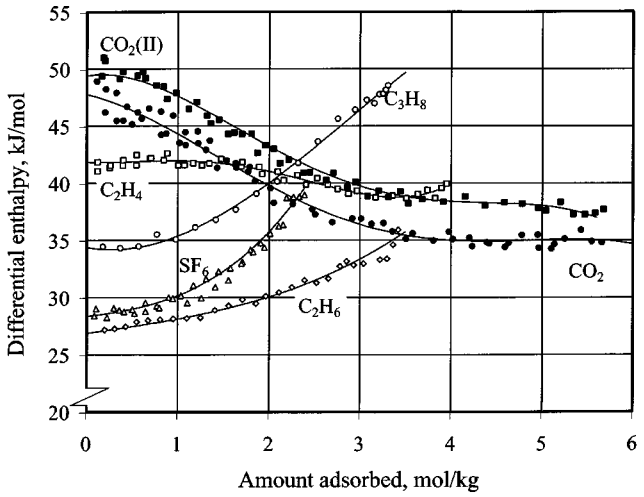

Figure 3. Experimental differential enthalpies (isosteric heats) on NaX at 298 K.

Solid lines are Eq. 35 with constants from Table 3.

for component Nos. 1 and 2 and perfect-gas behavior ($\phi_i = 1$) for our low-pressure measurements

$$Py_1 = P_1^\circ \gamma_1 x_1 \tag{39}$$

$$Py_2 = P_2^\circ \gamma_2 x_2 \tag{40}$$

are solved for the dependent variables P and y_1.

In summary, for each binary mixture point, there are seven equations (Eqs. 38, 39, 40 and two of Eqs. 34 and 37, one for each component) and seven unknowns (n_1°, n_2°, P_1°, P_2°, ψ, P, y_1). The equations may be solved consecutively as shown. In this way, the dependent variables (P, y_1) were calculated for the set of independent variables (n_1, n_2) and compared with experiment.

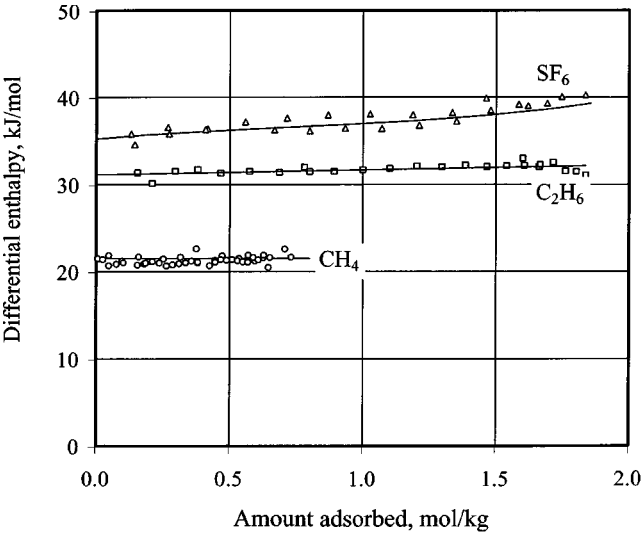

Figure 4. Experimental differential enthalpies (isosteric heats) on silicalite at 298 K.

Solid lines are Eq. 35 with constants from Table 3.

Table 3. Constants of Eq. 35 for Differential Enthalpies (Heats) of Desorption of Pure Gases at 25°C*

Gas	Zeolite	$\Delta\bar{h}^\circ$ kJ/mol	D_1	D_2	D_3	D_4	Error %
CO_2	NaX	47.776	−1.8994	−2.2273	0.7006	−0.0562	1.3
CO_2	NaX (II)	49.410	1.2389	−4.1093	1.1639	−0.0965	1.2
C_3H_8	NaX	34.400	−1.4850	2.7846	−0.3180	0.0	0.7
C_2H_4	NaX	41.836	−0.3215	1.2203	−0.9452	0.1576	0.7
C_2H_6	NaX	26.893	1.1719	−0.0328	0.1195	0.0	1.0
SF_6	NaX	28.368	0.9789	0.3086	0.5204	0.0	1.3
SF_6	Silicalite	35.908	1.8088	−3.4915	2.2187	0.0	1.6
C_2H_6	Silicalite	31.130	0.5581	0.0	0.0	0.0	1.0
CH_4	Silicalite	21.103	0.1924	0.0	0.0	0.0	1.5

*$\Delta\bar{h}$ is given in kJ/mol for n in mol/kg.

Calculation of dependent variables for a binary mixture presupposes knowledge of the values of two constants: C and $A_o = (A + BT)$. Values for C and A_o were extracted by minimizing the error in calculated values of pressure and selectivity (from Eq. 19), which set of variables is usually more sensitive than P and y_1 for the extraction of mixture parameters. Figure 5 shows a typical contour plot for the error in parameter space. After extracting parameters A_o and C for a binary mixture at a particular temperature, the values of A and B were determined by minimizing the error between the experimental differential enthalpies (heats) of desorption and the values calculated from Eqs. 20 and 27–30 under the constraint that $A_o = (A + BT)$. This two-step procedure is more effective than extracting values for all three constants at once by a simultaneous fit of mixture isotherms and enthalpies.

The ABC equation is more than an empirical fitting procedure because Eq. 24 has the asymptotic properties required by thermodynamics at low and high coverage (Talu and Myers, 1988; Talu et al., 1995). Since the ABC model is thermodynamically consistent, successful fitting of the model to the data implies that the experimental data are consistent as well. Thus, our experimental data obey all of the differential and integral thermodynamic consistency tests for binary mixtures (Valenzuela and Myers, 1989). In addition, our mixture data are consistent with the single-component isotherms at the limits $x_1 = 1$ and $x_2 = 1$.

Models with two parameters are unable to fit the data within experimental error. Models with four or more parameters can reduce the error, but the parameters begin to lose their physical significance. The three parameters in Eq. 24, which account for the excess enthalpy (A), the excess entropy (B), and the excess reciprocal loading (C), are necessary to describe mixture nonidealities as a function of temperature, composition, and loading. Values of these constants derived from experimental data for the binary mixtures are reported in Table 4. The most nonideal systems are polar-nonpolar pairs on NaX (CO_2-C_3H_8, CO_2-C_2H_6, C_2H_4-C_2H_6) and polar-polar pairs on NaX (CO_2-C_2H_4). Mixtures on nonpolar molecules of nearly the same size (C_2H_6-CH_4 in silicalite, SF_6-C_2H_6 in NaX) behave ideally as expected. Mixtures of nonpolar molecules of different size (SF_6-CH_4 in silicalite) exhibit nonidealities, but these entropic effects are weaker than the energetic effects observed for polar molecules in high electric fields.

Figures 6 and 7 show a comparison of the experimental and calculated pressure and gas-phase composition using the

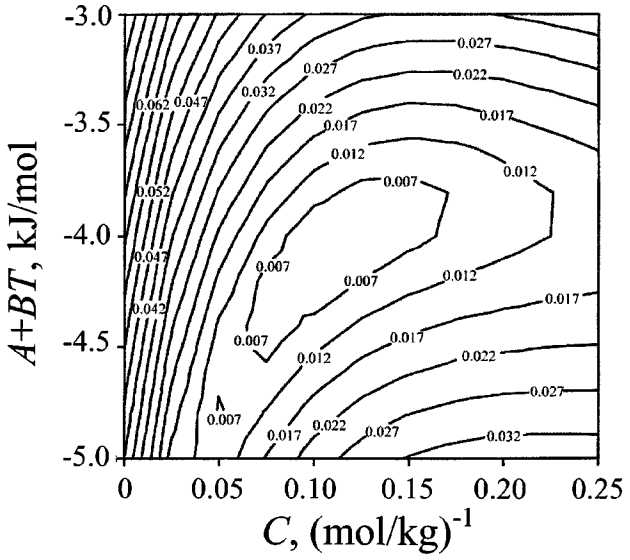

Figure 5. Contour lines for error in calculated pressure and selectivity plotted in parameter space for the binary mixture CO_2-C_2H_6 on NaX at 294 K using constants in Eq. 24.

The minimum error is located at $C = 0.11$ and $(A + BT) = -4.36$.

ABC equation for six systems: five nonideal mixtures and one ideal mixture (SF_6-C_2H_6 on NaX). The data for the ideal mixture CH_4-C_2H_6 on silicalite can be found elsewhere (Dunne et al., 1997). The error in the calculated pressure for four points of system A is large, but inconsistent with the other 21 points for which the average absolute error is 3%. The average absolute error in the calculated pressure for systems B, C, D, and E is 2%. The calculated pressures for system F are 9% too high but inconsistent with the nearly perfect agreement of experimental and calculated compositions for this system. The average absolute error in the calculated composition for all systems is 4%. Thus, the agreement of the ABC equation with experiment is generally excellent but there are systematic errors for systems A and F which would be difficult to explain even with a more complicated model.

The experimental differential enthalpies are larger than the ideal values, which is consistent with the negative deviations from ideal behavior observed for the selectivities. For example, heats of adsorption of CO_2 and C_2H_6 in a binary mixture are shown in Figure 8. The error in the IAS prediction

Table 4. Parameters of Eq. 24 for Adsorption of Binary Mixtures

Gases		Zeolite	A kJ/mol	B kJ/mol·K	C kg/mol
CO_2	C_3H_8	NaX	−11.5	0.01453	0.096
CO_2	C_2H_6	NaX	−10.0	0.01917	0.110
CO_2	C_2H_4	NaX	−6.5	0.01450	0.030
C_2H_4	C_2H_6	NaX	−4.5	0.00437	0.067
SF_6	CH_4	Silicalite	−1.8	0.00355	1.633
SF_6	C_2H_6	NaX	0.0	0.0	0.0
C_2H_6	CH_4	Silicalite	0.0	0.0	0.0

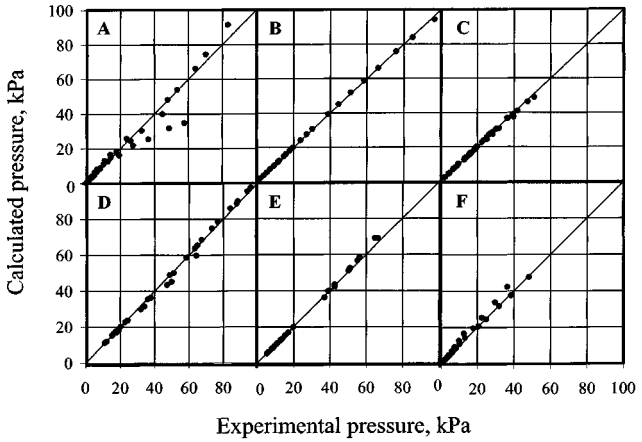

Figure 6. Experimental and calculated pressure for the binary systems.

(A) CO_2-C_3H_8 on NaX; (B) CO_2-C_2H_6 on NaX; (C) C_2H_4-C_2H_6 on NaX; (D) SF_6-CH_4 on silicalite; (E) SF_6-C_2H_6 on NaX; (F) CO_2-C_2H_4 on NaX.

increases with loading as expected. In spite of systematic errors of about 2 kJ/mol between the ABC equation and experiment, the fit is good considering that there is only one adjustable parameter (A) for the differential enthalpies of a binary mixture.

Ternary mixture

Ternary adsorption equilibria predicted from Eq. 33 using data for the three constituent binaries were compared with experiment for the system CO_2-C_2H_4-C_2H_6 on NaX. This system was selected because one of the binary pairs (CO_2-C_2H_6) is highly nonideal. The other two pairs are moderately nonideal (CO_2-C_2H_4 and C_2H_4-C_2H_6). Measurements are concentrated in the region of high loading where nonidealities are the strongest.

Figures 9, 10, and 11 compare calculated pressures, selectivities, and differential enthalpies, respectively, with experi-

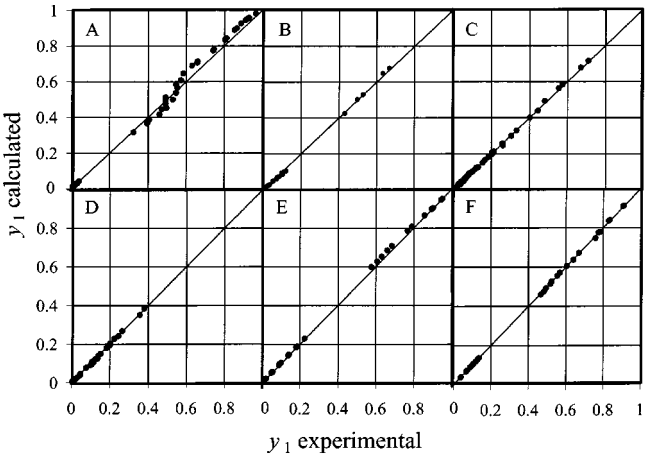

Figure 7. Experimental and calculated gas-phase composition for binary systems.

Legend: same as Figure 6.

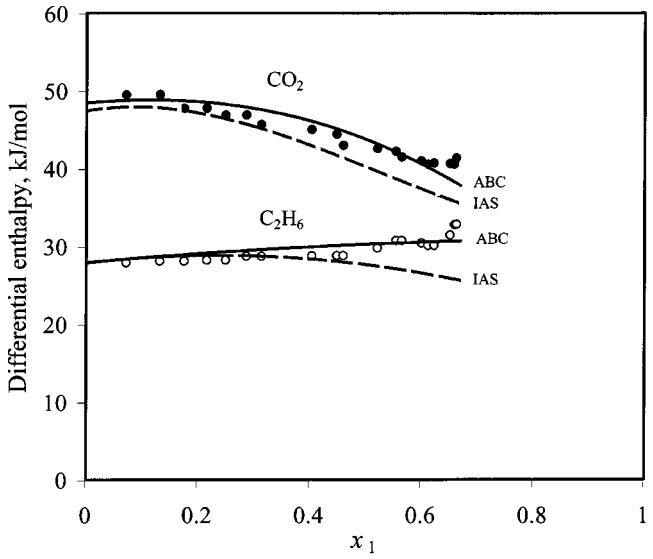

Figure 8. Experimental and calculated differential enthalpies (isosteric heats) for CO_2 and C_2H_6 on NaX.

Symbols are experimental values; solid lines are Eq. 20; dashed lines are Eq. 23 for IAS.

ment. The calculated pressure is 8% too high. The average absolute error in the selectivity is 12%. The average error in the calculated differential enthalpies is 2 kJ/mol, the same uncertainty observed for binary mixtures. Overall, agreement of experiment with the values calculated from Eq. 33 is good, but imperfect. Our analysis indicates that multicomponent equilibria can be predicted within about 10% from data for

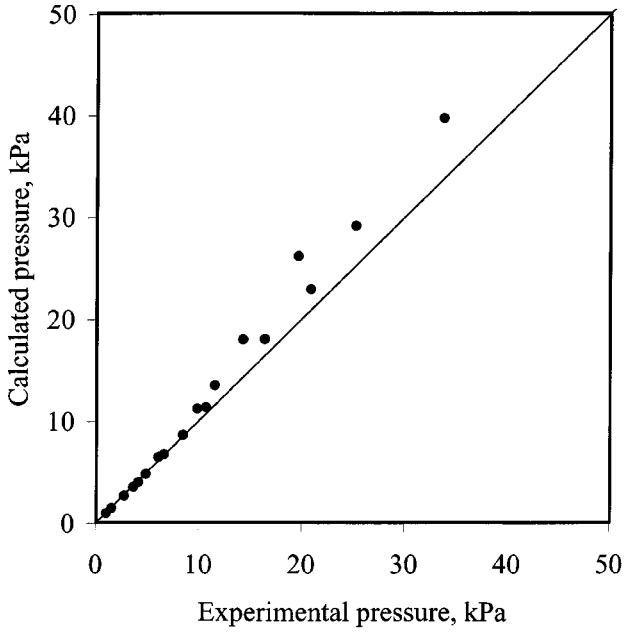

Figure 9. Comparison of experimental pressure for the ternary system CO_2-C_2H_4-C_2H_6 on NaX with pressure calculated from Eq. 33.

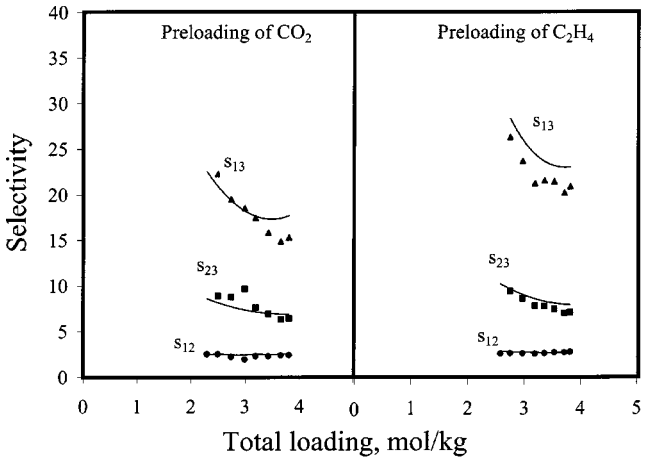

Figure 10. Comparison of experimental selectivity (points) for the ternary system CO_2 (1)-C_2H_4 (2)-C_2H_6 (3) on NaX with selectivity calculated from Eq. 33 (solid lines).

Selectivity $s_{ij} = (x_i y_j)/(x_j y_i)$.

the constituent binaries, but does not quite rule out the possibility of specific higher-order interactions.

Discussion

Isobaric phase diagrams

Isobaric, isothermal equilibrium diagrams have been used traditionally to represent binary adsorption data (Valenzuela and Myers, 1989). The constants of the ABC equation derived from fitting our experimental data over a wide range of conditions provide a means of calculating equilibrium diagrams as a function of temperature, pressure, and vapor-phase compositions. In the following discussion, we will refer to equilibrium diagrams calculated from the ABC equation

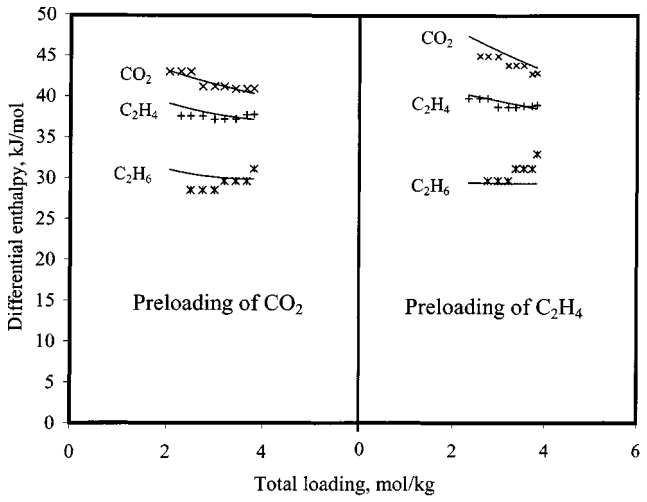

Figure 11. Comparison of experimental differential enthalpies (isosteric heats) for the ternary system CO_2-C_2H_4-C_2H_6 on NaX with enthalpies calculated from Eqs. 20 and 33.

as experimental data. Although these diagrams were not measured directly, they were calculated by correlating the experimental data with a thermodynamically consistent model.

Inversion of Eq. 34 for a pure component gives the function $n_i^\circ(P_i^\circ)$; substitution of $n_i^\circ(P_i^\circ)$ into Eq. 37 followed by another inversion gives the function $P_i^\circ(\psi)$. Having specified temperature (T), pressure (P), and vapor-phase mol fractions (y_i) as independent variables, substitution of the $P_i^\circ(\psi)$ functions into Eq. 9 yields a system of two equations in two unknowns (ψ and x_1). Isothermal, isobaric *xy* phase diagrams calculated this way are shown on Figure 12. The IAS prediction (dashed line) crosses the experimental data (solid line) at one point as required by thermodynamic consistency (Talu and Myers, 1988). The coverage at this pressure (13.3 kPa) corresponds to fairly high loading for all pure components except CH_4, as shown on Figures 1 and 2.

Figure 12 shows that the system CO_2-C_3H_8 on NaX is highly nonideal under these conditions and exhibits an azeotrope at about 80% CO_2. The compositions of the adsorbed and vapor phases are equal, but the pressure does not pass through a maximum at the azeotropic composition as would be the case for vapor-liquid equilibrium. For adsorption, isothermal *xy*-diagrams are a function of pressure. The system SF_6-C_2H_6 on NaX is ideal within experimental error, so the systems in Figure 12 display the full range of behavior from ideal to highly nonideal solutions.

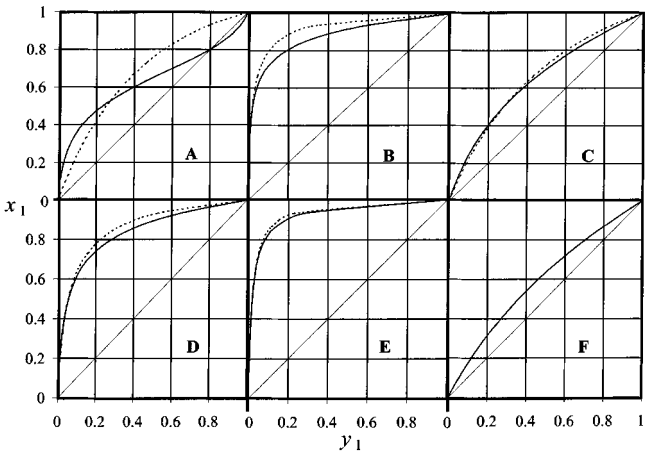

Figure 12. Isothermal (295 K), isobaric (13.3 kPa) *xy* diagrams.

(A) CO_2-C_3H_8 on NaX; (B) CO_2-C_2H_6 on NaX; (C) CO_2-C_2H_4 on NaX; (D) C_2H_4-C_2H_6 on NaX; (E) SF_6-CH_4 on silicalite; (F) SF_6-C_2H_6 on NaX. Dashed lines predicted by IAS theory.

Differential enthalpies at infinite dilution

Isothermal, isobaric, mixture differential enthalpies (heats) of adsorption are ploted on Figure 13. It is apparent that the experimental enthalpies (solid lines) are consistently higher than the values predicted by IAS (dashed lines), especially at infinite dilution. Substituting Eqs. 27–30 into Eq. 20 for infinite dilution ($x_i \to 0$ and $x_j \to 1$) gives

$$\Delta\bar{h}_i^\infty = \Delta h_i^\circ - A(1-e^{-C\psi}) + n_j^\circ\left(\Delta\bar{h}_j^\circ - \Delta h_j^\circ\right) \times\left(\frac{1}{n_i^\circ} + \frac{A+BT}{RT}Ce^{-C\psi}\right) \quad (41)$$

In the limit of high loading where deviations from ideal behavior are largest, ψ is large and the infinite dilution heats of adsorption at high loadings simplify to

$$\Delta\bar{h}_i^\infty = \Delta h_i^\circ - A + \frac{n_j^\circ}{n_i^\circ}\left(\Delta\bar{h}_j^\circ - \Delta h_j^\circ\right) \quad (42)$$

For an ideal solution, $A = 0$; for real solutions A is normally negative, corresponding to an exothermic enthalpy of mixing (see Table 4). Equation 42 agrees with Figure 13: experimental infinite-dilution enthalpies are larger than those predicted by IAS theory.

A rule of thumb is that a mixture differential enthalpy is given by the pure-component differential enthalpy at the same total loading. Is this rule better than IAS theory? Figure 14 shows a comparison of pure-component differential enthalpies (solid lines) with infinite-dilution enthalpies (dashed lines) for the system CO_2 and C_2H_6 in NaX. When the pure-component enthalpy increases with loading, as for C_2H_6, the infinite-dilution enthalpy is well represented by the pure-component enthalpy at the same loading as the *total* loading of the mixture, but for CO_2 in the same mixture, the infinite-dilution enthalpy is closer to the IAS prediction than to the pure-component enthalpy. Comparison of Figures 8 and 14 indicates that IAS theory is in general better than the rule of thumb for the prediction of differential enthalpies.

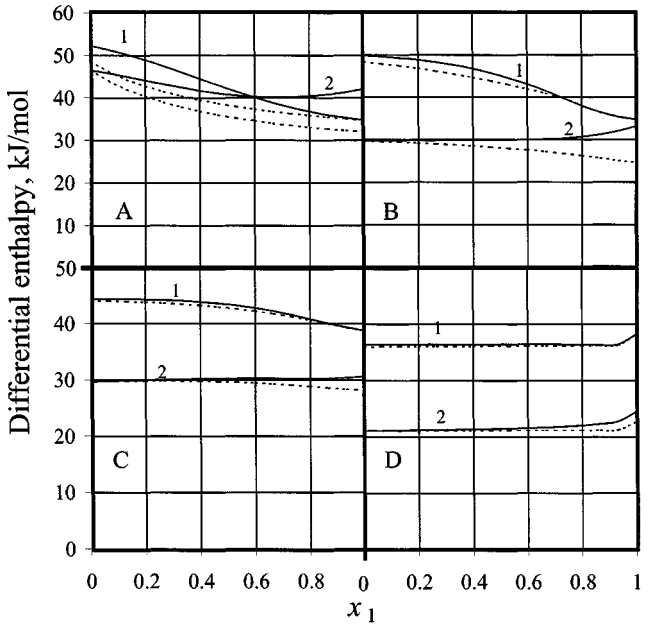

Figure 13. Isothermal (295 K), isobaric (13.3 kPa) differential enthalpies (isosteric heats).

(A) CO_2-C_3H_8 on NaX; (B) CO_2-C_2H_6 on NaX; (C) C_2H_4-C_2H_6 on NaX; and (D) SF_6-CH_4 on silicalite. Dashed lines predicted by IAS theory. Solid and dashed lines intersect at pure component enthalpies.

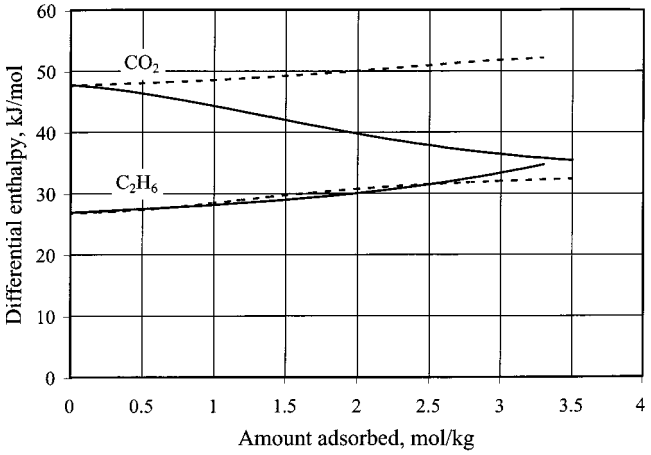

Figure 14. Comparison of infinite-dilution differential enthalpies (dashed lines) for the system CO_2-C_2H_6 on NaX at 298 K with pure-component heats of adsorption at the same *total* loading as the mixture (solid lines).

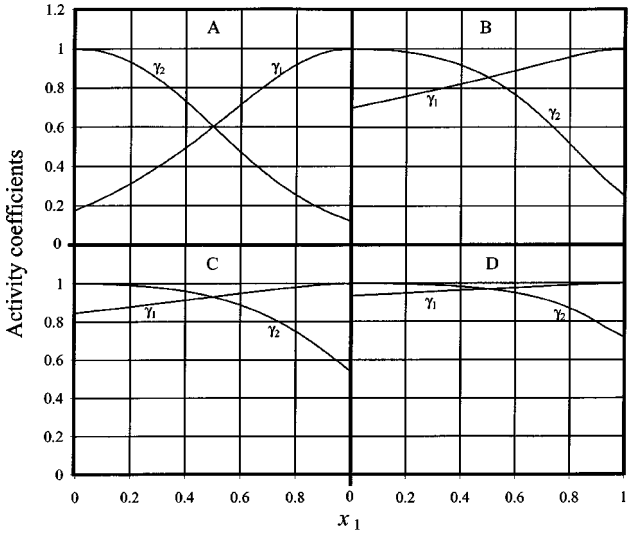

Figure 16. Isothermal (295 K), isobaric (13.3 kPa) activity coefficients.

x_1 is the mol fraction of the first component in the adsorbed phase. Legend: same as Figure 15.

Isobaric excess functions

The excess functions are useful for comparing deviations from ideality. Isobaric, isothermal excess functions are shown on Figure 15 and activity coefficients are shown on Figure 16, both for a constant pressure of 13.3 kPa. The excess enthalpy and excess free energy functions are negative. These negative deviations from Raoult's law generate activity coefficients which are less than unity. Since the excess enthalpy is always larger in absolute terms than the excess free energy, the idealisties in these systems are enthalpy driven. Entropic effects ($Ts^e = h^e - g^e$) are small but important.

Since Eq. 24 is quadratic in composition, the curves for the excess functions are symmetric at constant surface potential.

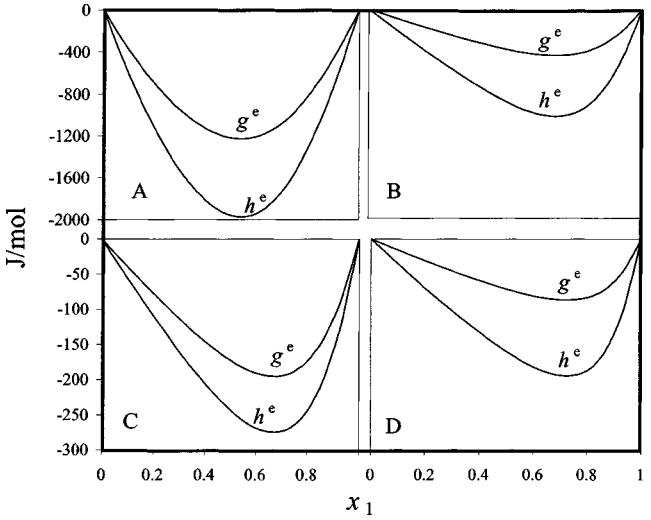

Figure 15. Isothermal (295 K), isobaric (13.3 kPa) excess enthalpy and excess free energy.

(A) CO_2-C_3H_8 on NaX; (B) CO_2-C_2H_6 on NaX; (C) C_2H_4-C_2H_6 on NaX; (D) SF_6-CH_4 on silicalite. x_1 is the mol fraction of the first component in the adsorbed phase.

Under the conditions of constant pressure imposed on Figures 15 and 16, the curves have their minima displaced towards the component with the higher loading (higher surface potential).

It is difficult to compare the relative magnitudes of the nonidealities on traditional isobaric plots because of large differences in their fractional coverages. To compare excess properties at the same fractional coverage, a saturation capacity of the mixture must be defined. Since $(1/n)^e \to 0$ at saturation, Eq. 17 gives

$$\frac{1}{m_{12}} = \frac{x_1}{m_1} + \frac{x_2}{m_2} \tag{43}$$

for the saturation capacity (m_{12}) of a binary mixture. The relative magnitudes of the nonidealities in the adsorbed phase are shown on Figures 17 and 18, where the excess free energy and the excess enthalpy are plotted as a function of coverage ($\theta = n_t/m_{12}$) for an equimolar composition in the adsorbed phase. One of the most interesting features of these figures is the similarity between h^e for the systems CO_2-C_3H_8 on NaX and CO_2-C_2H_6 on NaX in spite of large differences in g^e. This suggests that energetic effects are similar for mixtures of polar and nonpolar gases on an heterogeneous adsorbent, but entropic effects depend on the size and shape of the molecules. The quantity g^e/RT is dimensionless and may be compared with excess free energy functions for vapor-liquid equilibrium. The latter are usually positive while adsorption excess free energies are almost always negative. Liquid mixtures with positive free energies in the range above 0.5 are sufficiently nonideal to split into two liquid phases. Adsorbed solutions do not exhibit phase splitting because the excess free energies are negative, but the values of g^e/RT for the systems CO_2-C_3H_8 and CO_2-C_2H_6 on NaX place these systems into the highly nonideal category. The other binaries display moderate negative deviations from Raoult's law.

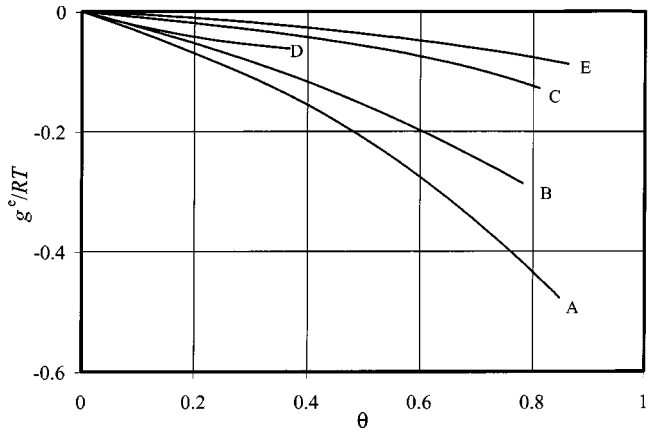

Figure 17. Dimensionless excess free energy as a function of fractional coverage (θ) at the equimolar composition ($x_1 = 0.5$).

(A): CO_2-C_3H_8 on NaX; (B): CO_2-C_2H_6 on NaX; (C): C_2H_4-C_2H_6 on NaX; (D): SF_6-CH_4 on silicalite; (E): CO_2-C_2H_4 on NaX.

Figure 17 shows that the excess free energy is negative for all of these systems. If one molecule has multiple sites with different energies, but the energy of adsorption of the other molecule is constant as for polar-nonpolar pairs adsorbed in faujasite, it has been shown the gas-solid energetic heterogeneity of the polar molecule generates negative deviations from Raoult's law (Myers, 1983) for the adsorbed mixture. For the systems studied here, this case is exemplified by the system CO_2-C_2H_6 on faujasite. If a larger molecule is denied access to some of the pores accessible to a smaller molecule, the effect of partial exclusion is to generate negative deviations from Raoult's law (Talu et al., 1995). Finally, if two molecules are substantially different in size, it has been shown by molecular simulation that the size difference generates small, but non-negligible, negative deviations from Raoult's law (Dunne and Myers, 1994). This case is exemplified by the system SF_6-CH_4 on silicalite. Positive deviations from Raoult's law stemming from gas-gas interactions in the adsorbed phase

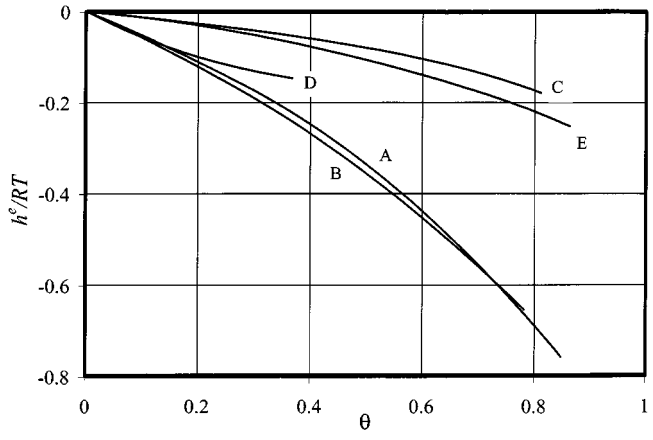

Figure 18. Dimensionless excess enthalpy as a function of fractional coverage (θ) at the equimolar composition ($x_1 = 0.5$).

Legend: same as Figure 17.

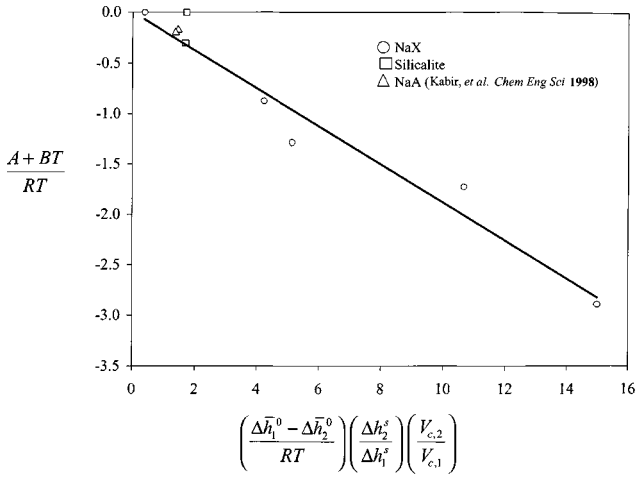

Figure 19. Correlation of constant $A_o = A + BT$ in Eq. 24 with pure-component properties.

$\Delta\bar{h}^\circ$ is the differential enthalpy of adsorption (isosteric heat) at the limit of zero loading; Δh^s is the molar integral enthalpy of adsorption from Eq. 36 evaluated at saturation; v_c is the critical volume of the gas.

have been observed for adsorption on a perfectly homogeneous surface such as graphitized carbon block (Friederich and Mullins, 1972), but not in complex heterogeneous materials such as zeolites and activated carbon in which gas-solid energetic, entropic, and exclusion effects predominate.

Correlation of excess functions

A major goal of this work is to develop a methodology for predicting nonideal mixture adsorption from pure-component properties. The important properties are: (a) the zero-coverage enthalpy and Henry constant, both of which characterize the interaction of a single molecule with the bare solid; (b) the integral enthalpy at saturation, which when compared to the zero-coverage enthalpy provides information of the energetic properties of the system; and (c) the critical volumes of the adsorbates for comparing the relative sizes of the molecules. Figure 19 shows a correlation for $A_o = A + BT$ with energetic and steric factors. The correlation captures well the trend for the systems studied, including an ideal system: SF_6-C_2H_6 on NaX, and a system studied by Kabir et al. (1998): CH_4-C_2H_6 on zeolite 5A. The log-log plot in Figure 20 shows that the constant C in Eq. 24 decreases with increasing saturation capacity of the mixture.

The linear correlations in Figures 19 and 20 are represented by

$$(A + BT) = -(0.188)\left(\frac{\Delta h_2^s}{\Delta h_1^s}\right)\left(\frac{V_{c2}}{V_{c1}}\right)\left(\Delta\bar{h}_1^\circ - \Delta\bar{h}_2^\circ\right) \quad (44)$$

and

$$C = \frac{31.8}{m_{12}^{3.96}} \quad (45)$$

Δh_i^s is the molar integral enthalpy of component i at saturation obtained by substituting the saturation capacity (m) from Table 2 into Eq. 36. $\Delta\bar{h}_i^\circ$ is the differential enthalpy at the

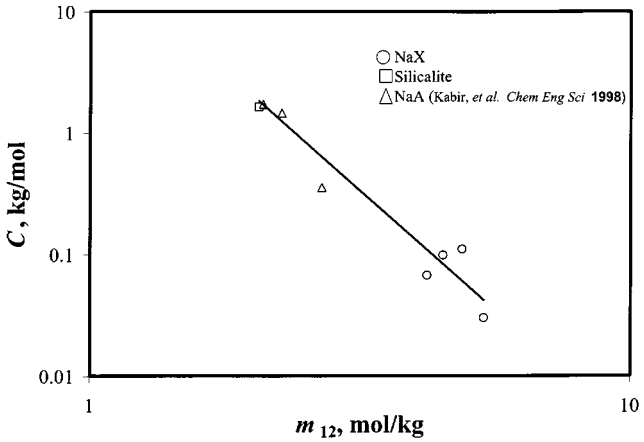

Figure 20. Correlation of constant *C* in Eq. 24 with pure-component properties.

m_{12} is the saturation capacity from Eq. 43.

limit of zero coverage (the value tabulated in Table 3). V_c is the critical volume of the gas. Component No. 1 is defined as the one with the larger value of $\Delta\bar{h}°$; consequently $(A + BT)$ in Eq. 44 is negative and has the same units as $\Delta\bar{h}°$. The constant C in Eq. 45 has units of kg/mol for m_{12} in mol/kg. The mixture saturation capacity m_{12} is calculated from Eq. 43 at the equimolar composition ($x_1 = 0.5$).

Equations 44 and 45 provide a means of predicting multicomponent adsorption equilibria from single-gas isotherms and enthalpies of adsorption. The effect of temperature upon the selectivity and loading is determined by the differential enthalpies (heats) of adsorption. Although the correlation is based on experimental data for only seven binaries and three types of zeolites, these systems cover a wide range of size differences and energetic effects. This correlation represents a first step toward the goal of predicting multicomponent mixture equilibria from single-component adsorption.

Conclusions

Isothermal measurements of adsorption equilibria and heats of adsorption describe the equilibrium behavior of mixtures as a function of temperature, pressure, and composition. Previous models of mixture adsorption were limited to isothermal systems; mixture enthalpies (heats) allow the effect of temperature to be introduced into the phase equilibrium calculations in a systematic way. The model proposed for the excess free energy in Eq. 24, along with single-component isotherms and enthalpies, provides a complete thermodynamic description of mixture adsorption for type I isotherms without hysteresis loops.

The sensitivity of mixture calculations to the accuracy of the single-gas measurements cannot be overemphasized.

Studies of the highly nonideal ternary system CO_2-C_2H_4-C_2H_6 on NaX indicate that the ternary data can be predicted with errors not exceeding 10% from data for the constituent binary systems.

The development of a correlation between the binary interaction parameters in Eq. 24 and pure component properties is a first step toward the goal of predicting multicomponent adsorption from single-gas adsorption isotherms and differential enthalpies (heats) of adsorption. The correlation, which accounts for entropic effects and energetic heterogeneity induced by differences in polarity, represents a major advancement over the theory of ideal adsorbed solutions (IAS).

The fact that mixture adsorption can be correlated in terms of single-gas isotherms and enthalpies is encouraging and suggests that accurate molecular models containing potential parameters extracted from single-gas data should be useful for predicting mixture adsorption by molecular simulation.

Acknowledgment

This research was supported by Air Products and Chemicals, Inc., and by National Science Foundation Grant NSF CTS 96-10030.

Literature Cited

Bajusz, I. G., J. G. Goodwin, Jr., D. Galloway, and N. Greenlay, "Isotopic Transient Study of Multicomponent N_2 and O_2 Adsorption on CaX Zeolite," *Langmuir*, **14**, 1846 (1998a).

Bajusz, I. G., J. G. Goodwin, Jr., D. Galloway, and N. Greenlay, "Effect of Ca^{2+} Exchange on Adsorption of N_2-O_2 Mixtures by NaCaX Zeolite," *Langmuir*, **14**, 2876 (1998b).

Bülow, M., "Determination of Sorption Thermodynamic Functions for Multi-Component Gas Mixtures Sorbed by Molecular Sieves," *Stud. Surf. Sci. Catal.*, **83**, 209 (1994).

Bülow, M., and D. Shen, "Sorption of Atmospheric Gases on a Faujasite-Type Zeolite—an Isosteric Investigation," *Fundamentals of Adsorption 6*, F. Meunier, ed., Elsevier, Paris, p. 87 (1998).

Crittenden, B. D., and W. J. Thomas, *Adsorption Technology & Design*, Butterworth-Heinemann, Woburn, MA (1998).

Dunne, J., and A. L. Myers, "Adsorption of Gas Mixtures in Micropores: Effect of Difference in Size of Adsorbate Molecules," *Chem. Eng. Sci.*, **49**, 2941 (1994).

Dunne, J. A., R. Mariwala, M. Rao, S. Sircar, R. J. Gorte, and A. L. Myers, "Calorimetric Heats of Adsorption and Adsorption Isotherms: 1. O_2, N_2, Ar, CO_2, CH_4, C_2H_6, and SF_6 on Silicalite," *Langmuir*, **12**, 5888 (1996a).

Dunne, J. A., M. Rao, S. Sircar, R. J. Gorte, and A. L. Myers, "Calorimetric Heats of Adsorption and Adsorption Isotherms: O_2, N_2, Ar, CO_2, CH_4, C_2H_6, and SF_6 on NaX, H-ZSM-5, and Na-ZSM-5 Zeolites," *Langmuir*, **12**, 5896 (1996b).

Dunne, J. A., M. Rao, S. Sircar, R. J. Gorte, and A. L. Myers, "Calorimetric Heats of Adsorption and Adsorption Isotherms: 3. Mixtures of CH_4 and C_2H_6 in Silicalite and Mixtures of CO_2 and C_2H_6 in NaX," *Langmuir*, **13**, 4333 (1997).

Friederich, R. O., and J. C. Mullins, "Adsorption Equilibria of Binary Hydrocarbon Mixtures on Homogeneous Carbon Black at 20°C," *Ind. Eng. Chem. Fundam.*, **11**, 439 (1972).

Golden, T. C., and S. Sircar, "Gas Adsorption on Silicalite," *J. Colloid Interface Sci.*, **162**, 182 (1994).

Hampson, J. A., and L. V. C. Rees, "Adsorption of Ethane and Propane in Silicalite-1 and Zeolite NaY: Determination of Single Component, Mixture and Partial Adsorption Data using an Isosteric System," *J. Chem. Soc., Faraday Trans.*, **89**, 3169 (1993).

Kabir, H., G. Grevillot, and D. Tondeur, "Equilibria and Activity Coefficients for Non-Ideal Adsorbed Mixtures from Perturbation Chromatography," *Chem. Eng. Sci.*, **53**, 1639 (1998).

Karavias, F., and A. L. Myers, "Isosteric Heats of Multicomponent Adsorption: Thermodynamics and Computer Simulations," *Langmuir*, **7**, 3118 (1991).

Meier, W. M., and D. H. Olson, *Atlas of Zeolite Structure Types*, Butterworth-Heinemann, 3rd ed., Stoneham, MA (1992).

Myers, A. L., "Activity Coefficients of Gas Mixtures Adsorbed on Heterogeneous Surfaces," *AIChE J.*, **29**, 691 (1983).

Myers, A. L., and J. M. Prausnitz, "Thermodynamics of Mixed-Gas Adsorption," *AIChE J.*, **11**, 121 (1965).

Prausnitz, J. M., R. N. Lichtenthaler, and E. Gomes de Azevedo, *Molecular Thermodynamics of Fluid-Phase Equilibria, Third Ed.*, Prentice-Hall, Upper Saddle River, NJ, pp. 213–299 (1999).

Rees, L. V. C., J. Hampson, and P. Brückner, "Sorption of Single Gases and Their Binary Mixtures in Zeolites," *Proc. of NATO Advanced Study Institute on Zeolite Microporous Solids: Synthesis,*

Structure and Reactivity, E. G. Derouane, F. Lemos, C. Naccache, and F. R. Ribeiro, eds., Kluwer Academic Publishers, Dordrecht, The Netherlands (1991).
Shen, D., M. Bülow, F. Siperstein, M. Englehard, and A. L. Myers, "Comparison of Experimental Techniques for Measuring Isosteric Heat of Adsorption," *Adsorption*, **6**, 275 (2000).
Siperstein, F., R. J. Gorte, and A. L. Myers, "A New Calorimeter for Simultaneous Measurements of Loading and Heats of Adsorption from Gaseous Mixtures," *Langmuir*, **15**, 1570 (1999a).
Siperstein, F., R. J. Gorte, and A. L. Myers, "Measurement of Excess Functions of Binary Gas Mixtures Adsorbed in Zeolites," *Adsorption*, **5**, 169 (1999b).
Sircar, S., "Excess Properties and Thermodynamics of Multicomponent Gas Adsorption," *J. Chem. Soc., Faraday Trans. 1*, **81**, 1527 (1985).
Sircar, S., "Isosteric Heats of Multicomponent Gas Adsorption on Heterogeneous Adsorbents," *Langmuir*, **7**, 3065 (1991).
Sircar, S., R. Mohr, C. Ristic, and M. B. Rao, "Isosteric Heats of Adsorption: Theory and Experiment," *J. Phys. Chem. B*, **103**, 6539 (1999).
Talu, O., and A. L. Myers, "Rigorous Thermodynamic Treatment of Gas Adsorption," *AIChE J.*, **34**, 1887 (1988).
Talu, O., J. Li, and A. L. Myers, "Activity Coefficients of Adsorbed Mixtures," *Adsorption*, **1**, 103 (1995).
Talu, O., "Needs, Status, Techniques and Problems with Binary Gas Adsorption Experiments," *Adv. Coll. Interface Sci.*, **76–77**, 227 (1998).
Tien, C., *Adsorption Calculations and Modeling*, Butterworth-Heinemann Series in Chemical Engineering, Butterworth-Heinemann, Woburn, MA (1994).
Valenzuela, D. P., and A. L. Myers, *Adsorption Equilibrium Data Handbook*, Prentice-Hall, Englewood Cliffs, NJ (1989).
Walas, S., *Phase Equilibria in Chemical Engineering*, Butterworth-Heinemann, Woburn, MA (1984).
Yang, R. T., *Gas Separation by Adsorption Processes*, Butterworths, Stoneham, MA (1987).

Appendix A

Equation 7 is a exact expression for the differential enthalpy of desorption, which is a generalized kind of isosteric heat for adsorption from real gas mixtures. The derivation of Eq. 7 requires consideration of the fundamental differential equations for the enthalpy and Gibbs free energy of an adsorbed fluid

$$dH^m = TdS^m + \sum_i \mu_i dn_i^m \tag{A1}$$

$$dG^m = -S^m dT + \sum_i \mu_i dn_i^m \tag{A2}$$

The quantities G^m, H^m, S^m, and n_i^m are Gibbs excess variables. The superscript m notation exphasizes that these variables are "measured" by experiment. In the following, the superscript is omitted for n_i^m to simplify the notation. The chemical potentials (μ_i) are set by the pressure, temperature, and composition of the equilibrium bulk gas. The absence of a VdP term is a consequence of the Gibbs definition of an adsorbed phase of zero excess volume. Using Eq. A1

$$\left(\frac{\partial H^m}{\partial n_i}\right)_{T,n_j} = T\left(\frac{\partial S^m}{\partial n_i}\right)_{T,n_j} + \mu_i \tag{A3}$$

A Maxwell-type equation for the differential entropy from Eq. A2 is

$$\left(\frac{\partial S^m}{\partial n_i}\right)_{T,n_j} = -\left(\frac{\partial \mu_i}{\partial T}\right)_{n_i,n_j} \tag{A4}$$

Combining Eqs. A3 and A4

$$\left(\frac{\partial H^m}{\partial n_i}\right)_{T,n_j} = \mu_i - T\left(\frac{\partial \mu_i}{\partial T}\right)_{n_i,n_j} = -T^2\frac{\partial}{\partial T}\left(\frac{\mu_i}{T}\right)_{n_i,n_j} \tag{A5}$$

Fugacity is defined by

$$\mu_i = \mu_i^* + RT\ln\frac{f_i}{f_i^*} \tag{A6}$$

where μ_i^* is the chemical potential in the perfect-gas reference state at which $f_i^* = 1$ bar. Substitution of Eq. A6 into A5 gives

$$\left(\frac{\partial H^m}{\partial n_i}\right)_{T,n_j} = -T^2\frac{d}{dT}\left(\frac{\mu_i^*}{T}\right) - RT^2\left(\frac{\partial \ln f_i}{\partial T}\right)_{n_i,n_j} \tag{A7}$$

From the thermodynamics of bulk fluids, the enthalpy and chemical potential in the perfect-gas reference state are related by

$$h_i^* = -T^2\frac{d}{dT}\left(\frac{\mu_i^*}{T}\right) \tag{A8}$$

so

$$\left(\frac{\partial H^m}{\partial n_i}\right)_{T,n_j} = h_i^* - RT^2\left(\frac{\partial \ln f_i}{\partial T}\right)_{n_i,n_j} \tag{A9}$$

Substituting the definition of differential enthalpy of desorption from Eq. 5 into Eq. A9 gives

$$\Delta\bar{h}_i = RT^2\left(\frac{\partial \ln f_i}{\partial T}\right)_{n_i,n_j} \tag{A10}$$

The differentiation, which is performed holding all mol numbers fixed, may be written

$$\Delta\bar{h}_i = RT^2\left(\frac{\partial \ln f_i}{\partial T}\right)_{n_1,n_2,\ldots} \qquad \text{Q.E.D.} \tag{A11}$$

Appendix B

Equation 20 is derived by differentiating the fugacity with respect to temperature while holding individual loadings (n_i) constant as prescribed by Eq. 7. Constant loading of all components is equivalent to constant total loading (n_t) and constant composition (x) so

$$\left(\frac{\partial \ln f_i}{\partial T}\right)_{n_1,n_2\ldots} = \left(\frac{\partial \ln f_i}{\partial T}\right)_{n_t,x} \tag{B1}$$

From the calculus

$$\left(\frac{\partial \ln f_i}{\partial T}\right)_{n_t,x} = \left(\frac{\partial \ln f_i}{\partial T}\right)_{\psi,x} + \left(\frac{\partial \ln f_i}{\partial \psi}\right)_{T,x}\left(\frac{\partial \psi}{\partial T}\right)_{n_t,x} \tag{B2}$$

From Eq. 9, the fugacity of the ith component in the adsorbed phase is

$$f_i = f_i^\circ x_i \gamma_i \tag{B3}$$

and

$$\ln f_i = \ln f_i^\circ + \ln x_i + \ln \gamma_i \tag{B4}$$

The derivative on the lefthand side of Eq. B2, which is not directly related to activity coefficients, has been expressed in terms of three other derivatives. Using Eq. B4, the first derivative on the righthand side of Eq. B2 may be expanded

$$\left(\frac{\partial \ln f_i}{\partial T}\right)_{\psi,x} = \left(\frac{\partial \ln f_i^\circ}{\partial T}\right)_{\psi} + \left(\frac{\partial \ln \gamma_i}{\partial T}\right)_{\psi,x} \tag{B5}$$

The pure-component derivative at constant ψ is related, but unequal, to the derivative at constant loading. From the calculus, for a pure component

$$\left(\frac{\partial \ln f}{\partial T}\right)_{\psi} = \left(\frac{\partial \ln f}{\partial T}\right)_{n} - \left(\frac{\partial \ln f}{\partial \psi}\right)_{T}\left(\frac{\partial \psi}{\partial T}\right)_{n} \tag{B6}$$

Temporarily, starting with Eq. B6, pure-component properties like f_i° are written without the subscript and superscript (f) to simplify the notation. Integration of Eq. 14 by parts gives

$$\psi = n \ln f - \int_0^n \ln f \, dn \qquad \text{(constant } T\text{)} \tag{B7}$$

so

$$\left(\frac{\partial \psi}{\partial T}\right)_{n} = n\left(\frac{\partial \ln f}{\partial T}\right)_{n} - \int_0^n \left(\frac{\partial \ln f}{\partial T}\right)_{n} dn \tag{B8}$$

The derivative $(\partial\psi/\partial T)_n$ is for single-component adsorption and, therefore, cannot be used in Eq. B2. From Eq. 14

$$\left(\frac{\partial \psi}{\partial \ln f}\right)_{T} = n \tag{B9}$$

Substitution of Eqs. B8 and B9 into B6 gives

$$\left(\frac{\partial \ln f}{\partial T}\right)_{\psi} = \left(\frac{\partial \ln f}{\partial T}\right)_{n} - \left(\frac{\partial \ln f}{\partial T}\right)_{n} + \frac{1}{n}\int_0^n \left(\frac{\partial \ln f}{\partial T}\right)_{n} dn \tag{B10}$$

Equation 7 for the differential enthalpy of a pure component is

$$\Delta \bar{h} = RT^2\left(\frac{\partial \ln f}{\partial T}\right)_{n} \tag{B11}$$

Substitution of Eq. B11 in B10 gives

$$\left(\frac{\partial \ln f}{\partial T}\right)_{\psi} = \frac{1}{nRT^2}\int_0^n \Delta \bar{h} \, dn \tag{B12}$$

Equation 6 for the molar integral enthalpy of a pure component is

$$\Delta h = \frac{\int_0^n \Delta \bar{h} \, dn}{n} \tag{B13}$$

Substitution of Eq. B13 in B12 gives

$$\Delta h = RT^2\left(\frac{\partial \ln f}{\partial T}\right)_{\psi} \tag{B14}$$

Comparison of Eq. B14 with B11 shows that the differential enthalpy is obtained by differentiation at constant loading, while the integral enthalpy is obtained by differentiation at constant ψ. Equations B6–B14 are for single-gas adsorption. The notation for pure-component reference states is now resumed, so that the integral enthalpy of pure component i is written Δh_i°. Substituting Eq. B14 in B5 gives

$$\left(\frac{\partial \ln f_i}{\partial T}\right)_{\psi,x} = \frac{\Delta h_i^\circ}{RT^2} + \left(\frac{\partial \ln \gamma_i}{\partial T}\right)_{\psi,x} \tag{B15}$$

Using Eq. B4, the second derivative on the righthand side of Eq. B2 is

$$\left(\frac{\partial \ln f_i}{\partial \psi}\right)_{T,x} = \left(\frac{\partial \ln f_i^\circ}{\partial \psi}\right)_{T} + \left(\frac{\partial \ln \gamma_i}{\partial \psi}\right)_{T,x} \tag{B16}$$

From Eq. 14 for a pure component in its reference state

$$\left(\frac{\partial \ln f_i}{\partial \psi}\right)_{T,x} = \frac{1}{n_i^\circ} + \left(\frac{\partial \ln \gamma_i}{\partial \psi}\right)_{T,x} \tag{B17}$$

Equation B17 shows that reciprocal loading $(1/n)$ arises naturally in the solution thermodynamics of adsorption. Defining an excess reciprocal loading variable by

$$(1/n)^e = \frac{1}{n_t} - \sum_i \frac{x_i}{n_i^\circ} \tag{B18}$$

the reciprocal of the total loading (n_t) may be written

$$\frac{1}{n_t} = \sum_i \frac{x_i}{n_i^\circ} + (1/n)^e \tag{B19}$$

The third derivative on the righthand side of Eq. B2 is the most difficult of the three derivatives to connect with excess properties. First, from the calculus

$$\left(\frac{\partial \psi}{\partial T}\right)_{n_t,x} = -\frac{\left(\frac{\partial (1/n_t)}{\partial T}\right)_{\psi,x}}{\left(\frac{\partial (1/n_t)}{\partial \psi}\right)_{T,x}} \tag{B20}$$

The third derivative on the righthand side of Eq. B2 has been rewritten as the ratio of two new derivatives, which are next evaluated using Eq. B19. The top derivative on the righthand side of Eq. B20 is

$$\left(\frac{\partial (1/n_t)}{\partial T}\right)_{\psi,x} = -\sum_i \frac{x_i}{(n_i^\circ)^2}\left(\frac{\partial n_i^\circ}{\partial T}\right)_{\psi} + \left(\frac{\partial (1/n)^e}{\partial T}\right)_{\psi,x} \tag{B21}$$

A brief digression is needed to evaluate the derivative of loading with respect to temperature at constant ψ for a pure

component. The notation will be simplified temporarily by omitting the superscript ° for a pure component. From the calculus

$$\left(\frac{\partial n}{\partial T}\right)_{\psi} = -\frac{\left(\frac{\partial \psi}{\partial T}\right)_{n}}{\left(\frac{\partial \psi}{\partial n}\right)_{T}} \tag{B22}$$

Substitution of Eq. B11 in B8 gives

$$\left(\frac{\partial \psi}{\partial T}\right)_{n} = \frac{n\Delta\bar{h}}{RT^2} - \frac{1}{RT^2}\int_0^n \Delta\bar{h}\,dn \tag{B23}$$

Using Eq. B13 for the definition of molar integral enthalpy, Eq. B23 reduces to

$$\left(\frac{\partial \psi}{\partial T}\right)_{n} = \frac{n(\Delta\bar{h} - \Delta h)}{RT^2} \tag{B24}$$

If the differential enthalpy of a pure adsorbate is constant with loading, then $h = \Delta\bar{h}$ and Eq. B24 predicts that ψ at fixed loading is independent of temperature.

A change of variables in Eq. 14 yields

$$\psi = \int_0^P n\,d\ln f = \int_0^n \left(\frac{\partial \ln f}{\partial \ln n}\right)_T dn \qquad \text{(constant } T\text{)} \tag{B25}$$

Therefore

$$\left(\frac{\partial \psi}{\partial n}\right)_T = \left(\frac{\partial \ln f}{\partial \ln n}\right)_T \tag{B26}$$

Substitution of Eqs. B24 and B26 into B22 gives

$$\left(\frac{\partial n}{\partial T}\right)_{\psi} = -\frac{n(\Delta\bar{h} - \Delta h)}{RT^2}\left(\frac{\partial \ln n}{\partial \ln f}\right)_T \tag{B27}$$

Returning to the notation of the mixture derivation for pure components which was temporarily suspended in Eqs. B22 to B27

$$\left(\frac{\partial n_i^\circ}{\partial T}\right)_{\psi} = -\frac{n_i^\circ\left(\Delta\bar{h}_i^\circ - \Delta h_i^\circ\right)}{RT^2}\left(\frac{\partial \ln n_i^\circ}{\partial \ln f_i^\circ}\right)_T \tag{B28}$$

Substitution of Eq. B28 in B21 gives the top derivative on the righthand side of Eq. B20

$$\left(\frac{\partial(1/n_t)}{\partial T}\right)_{\psi,x} = \sum_i \frac{x_i}{(n_i^\circ)^2}\left(\frac{n_i^\circ\left(\Delta\bar{h}_i^\circ - \Delta h_i^\circ\right)}{RT^2}\right) \times \left(\frac{\partial \ln n_i^\circ}{\partial \ln f_i^\circ}\right)_T + \left(\frac{\partial (1/n)^e}{\partial T}\right)_{\psi,x} \tag{B29}$$

Using Eq. B19, the bottom derivative on the righthand side of Eq. B20 is

$$\left(\frac{\partial(1/n_t)}{\partial \psi}\right)_{T,x} = -\sum_i \frac{x_i}{(n_i^\circ)^2}\left(\frac{\partial n_i^\circ}{\partial \psi}\right)_T + \left(\frac{\partial (1/n)^e}{\partial \psi}\right)_{T,x} \tag{B30}$$

Using Eq. B25

$$\left(\frac{\partial(1/n_t)}{\partial \psi}\right)_{T,x} = -\sum_i \frac{x_i}{(n_i^\circ)^2}\left(\frac{\partial \ln n_i^\circ}{\partial \ln f_i^\circ}\right)_T + \left(\frac{\partial (1/n)^e}{\partial \psi}\right)_{T,x} \tag{B31}$$

Substitution of Eqs. B29 and B31 into B20 gives the desired result for the third derivative on the righthand side of Eq. B2

$$\left(\frac{\partial \psi}{\partial T}\right)_{n_t,x} = \frac{\sum_i \frac{x_i}{(n_i^\circ)^2}\left(\frac{n_i^\circ\left(\Delta\bar{h}_i^\circ - \Delta h_i^\circ\right)}{RT^2}\right)\left(\frac{\partial \ln n_i^\circ}{\partial \ln f_i^\circ}\right)_T + \left(\frac{\partial (1/n)^e}{\partial T}\right)_{\psi,x}}{\sum_i \frac{x_i}{(n_i^\circ)^2}\left(\frac{\partial \ln n_i^\circ}{\partial \ln f_i^\circ}\right)_T - \left(\frac{\partial (1/n)^e}{\partial \psi}\right)_{T,x}} \tag{B32}$$

Defining a pure-component factor (G_i°) which is a function of the single-gas isotherm and its slope

$$G_i^\circ \equiv \frac{1}{(n_i^\circ)^2}\left(\frac{\partial \ln n_i^\circ}{\partial \ln f_i^\circ}\right)_T \tag{B33}$$

Equation B32 may be written

$$\left(\frac{\partial \psi}{\partial T}\right)_{n_t,x} = \frac{\sum_i x_i G_i^\circ n_i^\circ\left(\frac{\Delta\bar{h}_i^\circ - \Delta h_i^\circ}{RT^2}\right) + \left(\frac{\partial (1/n)^e}{\partial T}\right)_{\psi,x}}{\sum_i x_i G_i^\circ - \left(\frac{\partial (1/n)^e}{\partial \psi}\right)_{T,x}} \tag{B34}$$

Finally, substitution of Eqs. 7, B15, B17, and B34 into B2 gives

$$\Delta\bar{h}_i = \Delta h_i^\circ + RT^2\left(\frac{\partial \ln \gamma_i}{\partial T}\right)_{\psi,x} + \left[\frac{1}{n_i^\circ} + \left(\frac{\partial \ln \gamma_i}{\partial \psi}\right)_{T,x}\right] \times \left[\frac{\sum_j x_j G_j^\circ n_j^\circ\left(\Delta\bar{h}_j^\circ - \Delta h_j^\circ\right) + RT^2\left(\frac{\partial (1/n)^e}{\partial T}\right)_{\psi,x}}{\sum_j x_j G_j^\circ - \left(\frac{\partial (1/n)^e}{\partial \psi}\right)_{T,x}}\right]$$

Q.E.D. (B35)

Appendix C: Mixtures of CO_2 (1) and C_3H_8 (2) on NaX

Table C1. Mixtures of CO_2 (1) and C_3H_8 (2) on NaX

P kPa	n_t mol/kg	x_1	y_1	$s_{1,2}$	T °C	q_1 kJ/mol	q_2 kJ/mol
39.22	5.254	1.000	1.000		20.89		
47.91	5.351	0.969	0.966	1.12	20.92	34.18	38.49
53.48	5.431	0.970	0.966	1.15	20.91	33.02	38.01
64.05	5.492	0.946	0.930	1.32	21.19	33.03	38.40
70.20	5.554	0.948	0.929	1.38	21.35	34.52	39.22
83.22	5.589	0.927	0.888	1.61	21.48	34.70	41.83
3.01	2.967	1.000	1.000		20.76		
3.59	3.214	0.922	0.913	1.14	20.78	37.94	35.42
4.16	3.362	0.926	0.920	1.09	20.64	36.28	35.40
4.99	3.606	0.862	0.854	1.07	20.22	36.28	37.25
6.25	3.805	0.869	0.866	1.03	20.56	36.33	37.25
8.23	4.030	0.818	0.804	1.10	20.70	36.34	39.14
10.26	4.192	0.826	0.812	1.10	20.70	37.28	39.18
14.35	4.376	0.786	0.741	1.28	20.63	37.31	40.84
17.80	4.507	0.794	0.745	1.32	20.58	37.90	40.90
26.14	4.638	0.764	0.659	1.67	20.62	38.00	42.69
32.52	4.756	0.774	0.660	1.76	20.66	38.08	42.70
44.82	4.828	0.753	0.584	2.17	20.63	37.97	41.99
0.17	1.097	1.000	1.000		21.01		
0.33	1.350	0.813	0.547	3.59	21.02	44.21	35.29
0.44	1.586	0.841	0.631	3.08	21.06	42.86	35.29
0.61	1.835	0.726	0.493	2.73	21.03	42.86	36.65
0.79	2.072	0.758	0.572	2.34	21.06	42.47	36.65
1.01	2.325	0.675	0.491	2.15	21.03	42.47	37.50
1.22	2.541	0.703	0.555	1.90	20.25	42.64	37.50
1.55	2.794	0.639	0.493	1.82	20.35	42.64	39.10
1.96	3.006	0.665	0.547	1.64	20.41	41.29	39.10
2.78	3.254	0.613	0.498	1.60	20.39	41.30	41.02
3.37	3.453	0.636	0.530	1.55	20.44	42.90	41.04
5.05	3.689	0.594	0.460	1.72	20.43	42.93	43.78
6.54	3.851	0.613	0.474	1.76	20.39	42.40	43.77
10.97	4.035	0.582	0.396	2.13	20.37	42.47	45.48
14.19	4.162	0.599	0.406	2.19	20.36	43.83	45.57
23.83	4.280	0.578	0.325	2.85	20.31	43.62	43.85
2.68	2.526	0.000	0.000		20.74		
3.45	2.768	0.090	0.010	9.81	20.75	51.56	42.49
5.48	2.931	0.085	0.010	9.21	20.77	51.62	44.57
8.30	3.150	0.157	0.020	9.13	20.73	50.93	44.56
12.90	3.255	0.152	0.018	9.76	20.38	51.09	46.09
19.31	3.410	0.207	0.028	9.06	20.53	48.88	46.08
27.49	3.465	0.203	0.024	10.38	20.83	48.80	45.77
36.39	3.584	0.251	0.037	8.73	20.99	47.29	45.74
48.67	3.623	0.248	0.032	9.98	20.94	46.34	43.31
57.75	3.720	0.288	0.041	9.48	20.94	45.29	43.26

Table C2. Mixtures of SF_6 (1) and C_2H_6 (2) on NaX

P kPa	n_t mol/kg	x_1	y_1	$s_{1,2}$	T °C	q_1 kJ/mol	q_2 kJ/mol
34.52	2.859	0.000	0.000		20.79		
39.17	2.927	0.030	0.022	1.38	20.82	37.00	33.57
42.66	2.981	0.030	0.021	1.42	21.07	36.90	33.18
51.19	3.062	0.067	0.057	1.19	21.14	37.06	33.18
55.18	3.106	0.066	0.055	1.21	21.18	37.22	33.71
66.59	3.171	0.100	0.090	1.13	21.26	38.69	33.74
32.29	2.157	1.000	1.000		20.69		
37.08	2.239	0.957	0.946	1.26	20.72	37.11	33.68
42.81	2.292	0.958	0.950	1.20	20.95	37.76	33.78
50.34	2.388	0.910	0.894	1.19	21.16	37.77	34.67
56.35	2.434	0.911	0.902	1.12	21.33	37.78	34.67
64.82	2.515	0.871	0.857	1.13	21.40	37.78	34.24
7.54	1.126	0.000	0.000		20.74		
8.44	1.271	0.116	0.052	2.39	20.87	31.07	28.48
9.28	1.371	0.108	0.049	2.34	21.04	31.09	29.28
10.39	1.511	0.193	0.101	2.12	21.10	31.76	29.28
11.40	1.613	0.180	0.095	2.10	21.14	31.76	29.55
12.88	1.751	0.247	0.143	1.97	21.16	32.52	29.55
13.83	1.827	0.237	0.140	1.91	21.20	32.55	30.59
15.87	1.963	0.292	0.186	1.81	21.26	33.17	30.60
17.05	2.034	0.282	0.180	1.79	21.32	33.22	31.86
19.72	2.164	0.329	0.225	1.69	21.35	34.27	31.87
3.99	0.951	1.000	1.000		18.82		
5.42	1.241	0.884	0.766	2.32	18.79	30.70	29.07
6.23	1.347	0.893	0.789	2.23	18.84	30.77	29.07
7.93	1.489	0.807	0.660	2.15	18.92	30.77	29.89
9.02	1.584	0.819	0.685	2.08	18.99	32.67	29.92
11.17	1.727	0.749	0.606	1.94	19.09	32.68	30.84
12.72	1.813	0.762	0.631	1.87	19.22	33.29	30.85
15.33	1.944	0.708	0.576	1.79	19.27	33.29	31.02

Table C3. Mixtures of SF_6 (1) and CH_4 (2) on Silicalite

P kPa	n_t mol/kg	x_1	y_1	$s_{1,2}$	T °C	q_1 kJ/mol	q_2 kJ/mol
2.08	0.651	1.000	1.000		21.00	35.14	22.57
11.34	0.720	0.903	0.201	36.87	21.05	36.74	22.60
12.18	0.814	0.917	0.225	37.96	21.21	36.74	22.39
22.99	0.880	0.845	0.138	34.05	21.36	35.74	22.35
24.43	0.970	0.865	0.152	35.54	21.44	35.76	22.66
36.01	1.029	0.812	0.116	32.90	21.53	35.67	22.66
37.79	1.102	0.833	0.126	34.76	21.49	35.62	22.19
48.83	1.155	0.792	0.107	31.77	21.49	35.91	22.21
51.29	1.224	0.815	0.114	34.10	21.50	35.98	22.71
63.37	1.273	0.781	0.101	31.80	21.49		
15.32	0.287	0.528	0.020	54.28	21.30		
16.25	0.442	0.700	0.048	46.61	21.29		
17.44	0.596	0.784	0.078	43.01	21.46		
18.79	0.735	0.830	0.110	39.61	21.55		
20.40	0.865	0.861	0.143	37.12	21.76		
5.77	1.020	1.000	1.000		25.09	37.56	23.34
17.88	1.076	0.944	0.357	30.52	25.11	36.60	23.28
19.19	1.145	0.950	0.380	30.96	25.09	36.54	21.69
32.12	1.194	0.908	0.245	30.42	25.21	36.81	21.71
34.06	1.257	0.917	0.265	30.72	25.17	36.91	22.92
47.35	1.296	0.886	0.202	30.70	25.23	37.27	22.95
49.99	1.352	0.897	0.222	30.42	25.28	37.31	23.32
64.33	1.391	0.868	0.184	29.30	25.31		
56.02	0.424	0.000	0.000		24.11	39.43	21.28
58.36	0.565	0.271	0.008	47.88	24.16	39.43	21.17
64.79	0.602	0.255	0.007	47.76	24.25	38.22	21.17
67.30	0.726	0.400	0.015	44.06	24.28	38.22	21.23
73.38	0.757	0.383	0.014	43.07	24.32	37.75	21.23
76.77	0.884	0.491	0.024	39.43	24.37	37.72	20.99
83.99	0.916	0.474	0.022	39.45	24.39	37.87	20.99
88.42	1.038	0.556	0.034	35.81	24.39	37.98	21.74
95.86	1.065	0.541	0.032	35.55	24.36	39.03	21.76
101.56	1.180	0.609	0.046	32.54	24.41	39.17	22.52
108.96	1.203	0.596	0.044	31.92	24.35		
84.49	0.583	0.000	0.000		24.42	36.02	20.08
87.81	0.706	0.200	0.005	46.56	24.56	36.11	20.79
93.91	0.735	0.192	0.005	49.93	24.75	36.44	20.79
98.09	0.862	0.335	0.012	42.11	24.98	36.63	22.07
104.72	0.889	0.325	0.011	43.00	25.14	37.71	22.07
109.99	0.972	0.412	0.018	38.35	25.12		

Table C4. Mixtures of C_2H_4 (1) and C_2H_6 (2) on NaX

P kPa	n_t mol/kg	x_1	y_1	$s_{1,2}$	T °C	q_1 kJ/mol	q_2 kJ/mol
7.45	2.877	1.000	1.000		23.92	39.05	30.22
12.77	3.047	0.941	0.670	7.81	23.94	39.50	30.24
16.76	3.221	0.946	0.710	7.13	24.10	39.57	32.12
25.22	3.363	0.900	0.553	7.28	24.17	40.61	32.24
28.51	3.433	0.904	0.574	7.03	24.26	40.77	33.46
39.71	3.545	0.869	0.481	7.14	24.22		
1.60	1.824	1.000	1.000		24.43	41.69	28.78
4.29	2.037	0.895	0.402	12.65	24.49	41.20	28.76
4.83	2.171	0.902	0.444	11.50	24.78	41.21	30.55
7.73	2.352	0.832	0.304	11.33	24.94	40.55	30.57
8.64	2.471	0.841	0.333	10.63	25.10	40.16	31.09
13.05	2.671	0.777	0.260	9.90	25.15	40.11	31.09
13.91	2.718	0.783	0.258	10.37	25.14	40.06	30.72
18.65	2.909	0.731	0.204	10.58	24.29	40.42	30.72
19.26	2.937	0.734	0.213	10.20	24.34	40.60	32.53
26.52	3.106	0.692	0.185	9.88	24.46	40.10	32.51
27.26	3.125	0.695	0.187	9.92	24.54	40.42	33.98
36.39	3.266	0.663	0.167	9.79	24.87		
0.43	0.967	1.000	1.000		24.17	41.03	27.00
2.16	1.164	0.830	0.203	19.20	24.24	39.10	27.00
2.19	1.202	0.836	0.210	19.14	24.28	39.11	28.03
4.14	1.410	0.712	0.114	19.35	24.41	37.69	28.03
4.22	1.456	0.722	0.120	19.01	24.47	37.70	29.36
6.63	1.686	0.623	0.081	18.73	24.54	38.39	29.36
6.77	1.738	0.635	0.083	19.18	24.62	38.41	30.29
9.39	1.956	0.563	0.067	17.96	24.67	39.12	30.29
9.65	2.017	0.577	0.074	17.09	24.64		
12.98	1.937	0.390	0.041	14.94	26.00	42.90	31.87
13.77	1.988	0.380	0.037	15.80	26.10	43.02	31.87
15.51	2.223	0.452	0.054	14.44	26.18	43.03	32.21
16.43	2.276	0.442	0.048	15.65	26.10	43.53	32.20
18.94	2.506	0.501	0.066	14.28	26.06	43.47	31.54
19.90	2.547	0.492	0.062	14.68	25.90	42.57	31.54
23.52	2.766	0.543	0.082	13.28	25.83	42.39	30.00
25.18	2.814	0.533	0.077	13.70	25.76	42.07	30.00
30.24	3.005	0.575	0.103	11.79	25.71	41.95	29.30
31.97	3.046	0.567	0.098	12.06	24.46	42.04	29.31
39.06	3.208	0.604	0.130	10.21	25.60	42.01	29.18
41.93	3.240	0.598	0.122	10.76	25.83	41.66	29.17
51.09	3.378	0.632	0.154	9.45	25.95		
13.63	1.783	0.000	0.000		21.11	43.54	30.23
15.14	2.040	0.133	0.007	23.37	21.13	43.65	32.35
16.01	2.096	0.129	0.007	21.01	21.28	43.50	32.36
18.23	2.340	0.228	0.015	19.67	21.45	43.52	32.58
19.36	2.394	0.223	0.015	18.84	21.69	43.08	32.58
22.54	2.624	0.302	0.022	19.16	21.79	43.05	32.30
23.88	2.673	0.296	0.021	19.48	21.83	43.91	32.31
28.37	2.882	0.361	0.029	19.10	21.85	44.17	33.90
30.55	2.936	0.354	0.029	18.17	21.80	44.41	33.90
36.83	3.117	0.410	0.040	16.74	21.70		
39.29	3.155	0.404	0.041	15.85	21.62		
47.46	3.305	0.453	0.055	14.13	21.53		

Table C5. Mixtures of CO_2 (1) and C_2H_4 (2) on NaX

P kPa	n_t mol/kg	x_1	y_1	$s_{1,2}$	T °C	q_1 kJ/mol	q_2 kJ/mol
0.63	1.718	1.000	1.000		23.94	44.13	38.23
0.99	1.939	0.886	0.759	2.46	23.99	42.49	38.22
1.32	2.157	0.897	0.782	2.44	24.01	42.49	37.40
1.93	2.387	0.810	0.641	2.39	24.10	41.29	37.39
2.49	2.616	0.827	0.671	2.35	24.13	41.29	37.26
3.47	2.855	0.757	0.568	2.37	24.10	40.57	37.25
4.40	3.092	0.776	0.604	2.28	24.10	40.57	37.37
5.98	3.337	0.718	0.525	2.30	24.03	41.44	37.38
7.43	3.576	0.738	0.555	2.26	23.80	41.45	37.74
9.96	3.805	0.692	0.495	2.29	23.80	40.11	37.70
12.49	4.029	0.711	0.518	2.29	23.89	40.10	37.61
16.73	4.236	0.673	0.467	2.35	23.96	40.62	37.65
20.63	4.422	0.691	0.485	2.37	23.97		
15.98	4.465	1.000	1.000		20.54	37.61	36.64
20.63	4.646	0.955	0.907	2.19	20.54	38.01	36.69
24.85	4.800	0.957	0.911	2.19	20.56	38.01	36.93
32.05	4.951	0.920	0.831	2.34	20.62	38.10	36.95
38.38	5.086	0.924	0.836	2.38	20.72	38.14	37.65
48.22	5.200	0.894	0.775	2.44	20.75		
1.89	1.999	0.000	0.000		23.46	44.42	40.86
2.53	2.239	0.109	0.042	2.80	23.47	44.39	39.28
3.44	2.465	0.099	0.038	2.79	23.49	43.59	39.28
4.56	2.706	0.183	0.075	2.76	23.45	43.58	39.00
6.26	2.939	0.168	0.069	2.72	23.43	42.61	38.99
8.08	3.169	0.233	0.101	2.70	23.38	42.56	38.28
10.24	3.382	0.218	0.090	2.81	21.75	42.99	38.29
13.26	3.605	0.273	0.118	2.80	21.66	42.97	38.08
17.73	3.779	0.259	0.108	2.89	21.64	42.61	38.08
22.42	3.966	0.303	0.129	2.94	21.64	42.67	38.44
29.63	4.105	0.291	0.120	3.02	21.70	42.75	38.45
36.46	4.260	0.330	0.136	3.13	21.71		

Table C6. Mixtures of CO_2 (1) and C_2H_6 (2) on NaX

P kPa	n_t mol/kg	x_1	y_1	$s_{1,2}$	T °C	q_1 kJ/mol	q_2 kJ/mol
6.38	3.532	1.000	1.000		20.76	38.23	28.99
10.62	3.717	0.949	0.633	10.81	20.76	38.39	29.00
12.61	3.924	0.953	0.666	10.09	20.67	38.41	30.37
18.22	4.087	0.913	0.498	10.55	20.63	38.33	30.36
21.43	4.274	0.919	0.528	10.13	20.64	38.35	30.85
28.65	4.406	0.889	0.431	10.54	20.61		

Table C7. Ternary Equilibrium Data

P, torr	n_t mol/kg	x_{CO_2}	$x_{C_2H_4}$	$x_{C_2H_6}$	y_{CO_2}	$y_{C_2H_4}$	$y_{C_2H_6}$
7.35	2.054	1.000	0.000	0.000	1.000	0.000	0.000
11.41	2.297	0.893	0.107	0.000	0.768	0.232	0.000
30.91	2.498	0.821	0.098	0.081	0.287	0.086	0.627
36.35	2.744	0.838	0.089	0.073	0.342	0.081	0.577
45.41	2.993	0.768	0.167	0.065	0.334	0.140	0.526
73.62	3.193	0.719	0.156	0.125	0.221	0.110	0.669
86.18	3.428	0.741	0.145	0.114	0.257	0.115	0.628
106.66	3.657	0.693	0.202	0.105	0.254	0.175	0.571
147.18	3.810	0.664	0.194	0.142	0.201	0.140	0.659
20.37	2.337	0.000	1.000	0.000	0.000	1.000	0.000
27.36	2.578	0.097	0.903	0.000	0.041	0.959	0.000
49.38	2.753	0.090	0.845	0.065	0.024	0.577	0.399
63.27	2.970	0.084	0.857	0.059	0.025	0.625	0.350
80.12	3.192	0.153	0.793	0.054	0.048	0.635	0.317
122.77	3.357	0.146	0.751	0.103	0.035	0.477	0.488
156.32	3.531	0.138	0.768	0.094	0.034	0.515	0.451
189.04	3.712	0.190	0.724	0.086	0.050	0.528	0.422
252.99	3.817	0.185	0.698	0.117	0.042	0.449	0.509

Table C8. Ternary Heats of Adsorption

n_t mol/kg	x_{CO_2}	$x_{C_2H_4}$	$x_{C_2H_6}$	q_{CO_2}	$q_{C_2H_4}$	$q_{C_2H_6}$
2.054	1.000	0.000	0.000	42.99		
2.175	0.947	0.053	0.000	42.99	37.53	
2.283	0.905	0.068	0.027	42.99	37.53	28.45
2.513	0.851	0.098	0.051	41.16	37.52	28.45
2.745	0.809	0.118	0.073	41.16	37.13	28.45
2.977	0.774	0.138	0.088	41.17	37.15	29.56
3.205	0.743	0.156	0.101	40.87	37.14	29.56
3.426	0.717	0.168	0.115	40.88	37.71	29.57
3.632	0.700	0.180	0.120	40.92	37.76	31.07
2.337	0.000	1.000	0.000		39.84	
2.457	0.048	0.952	0.000	45.06	39.84	
2.556	0.062	0.916	0.022	45.06	39.84	29.68
2.767	0.090	0.869	0.041	45.02	38.78	29.66
2.972	0.109	0.832	0.059	43.91	38.78	29.66
3.173	0.127	0.801	0.072	43.94	38.80	31.19
3.360	0.146	0.770	0.084	43.95	38.92	31.20
3.533	0.158	0.747	0.095	42.86	38.91	31.20
3.687	0.171	0.730	0.099	42.98	39.05	32.99

Manuscript received Nov. 18, 1999, and revision received Aug. 23, 2000.